AQUIFER VULNERABILTY ASSESSEMNET AROUND A MAJOR DUMPSITE LOCATED WITHIN GOSHEN CITY IN NASARAWA STATE USING INTEGRATED GEOPHYSICAL METHODS

ABSTRACT

This study combined geophysical (VES, 2-D ERT, SP, VLF-EM) methods to evaluate the extent of leachate migration into aquifer systems within a major dumpsite located within the Goshen City in Nasarawa State. The geology of the area situated between latitude ($8^0$56$^{'}$8.0874''N and $8^0$56$^{'}$8.232'' N) and longitude ($7^0$40$^{'}$ 52.1178$^{''}$ E and $7^0$40$^{'}$35.241$^{''}$ E) consists of basement complex and sedimentary rocks. A total of fifteen VES points, three 2-D ERT profiles, ten SP profiles, and ten VLF transverses were created within the dumpsite and the control site. The geophysical data collected with the aid of Ohmega Allied resistivity meter and portable Gem VLF receiver were interpreted with WinResist, RES2DINV, Grapher, Surfer and KHFFILT softwares. The geophysical methods identified zones of groundwater saturation and potential contamination pathways (e.g., fractures, faults) within the study area. The results revealed five to six discrete layers, such as the Topsoil (lateritic), clayey sand, sandy silt, weathered/fractured and fresh bedrocks. Materials with low resistivity values ranging from (1.6 to 35.3 Ω.m, extending to depths ≥ 98 m) along the transverses were delineated as leachate infiltrated zones. These zones were dominated by negative SP anomalies ranging from (-578 to -2.4 mV), attributed to differences in mobility and concentration of ions emanating from percolated organic and inorganic materials from the dumpsite, in contrast to dominant positive SP anomalies ranging from (1.8 to 247 mV) recorded at the control site. This suggested that the control site was devoid of leachate contaminants. Objects with positive VLF current-density ranging from (5 to 10 %) extending to depths of 15 m along the profiles, were interpreted as electrical conducting paths generated by leachate contaminants. The Aquifer Protective Capacity ranged from poor to excellent, with VES 7 (30.18 S) representing (6.7%) rated as excellent; two (2) VES points; VES 1 (0.27 S) and VES 5 (0.31 S) representing (13.3 %) were rated as moderate; VES 4 (0.153 S), VES 9 (0.155 S), and VES 14 (0.14 S) representing (20 %) were rated as weak, while, VES 8 (0.066 S), VES 6 (0.061 S), VES 3 (0.053 S), VES 11 (0.044 S), VES 2 (0.027 S), VES 10 (0.0075 S), VES 13 (0.0063 S), VES 12 (0.0044 S), VES 15 (0.00046 S), representing 60 % of the sounding points, showed poor protective capacity rating. The findings reveal that the study area lacks adequate impervious clay-seals necessary to safeguard groundwater resources from leachate infiltration. The installation of geo-synthetic clay liners at the base of the dumpsites and continuous monitoring are recommended for effective waste disposal management.

Keywords: Leachate, aquifer vulnerability, aquifer protective capacity, resistivity, self-potential

1.1 INTRODUCTION

The steady influx of people into the Goshen City in Karu LGA, Nasarawa State in search of greener pasture has resulted in the generation of substantial solid wastes stemming from diverse sources (domestic and industrial) [13]. The poor disposal of this wastes without recourse to engineering considerations, generate leachate which become point source of pollution into surrounding soils and groundwater [8, 1]. The solid waste from this dumping process undergoes slow, anaerobic decomposition over a period of years and generate substantial amount of leachate with

decomposing products such as leachate, landfill gas, heavy metals and varieties of hazardous pollutants which may seep from the dumpsite into underground aquifer systems [1]. The present study integrated geophysical methods to conduct aquifer vulnerability assessment around a major open dumpsite in Goshen City, Nasarawa State, with a view to providing an efficient policy formulation guide for effective waste disposal management.

2.1 REVIEW OF LITERATURE

The electrical properties of leachate substantially aid in the use of integrated geo-electrical and E-M methods such as VES, 2-D ERT, SP and VLF-EM methods [18] in delineating their extent of migration into the subsurface. In light of this, [6] assessed the extent of leachate infiltration from waste dumpsite into groundwater resources at Gyadi-Gyadi, Kano State, Nigeria, using natural Electromagnetic (EM) field and VES methods. Results revealed leachate-aquifer interaction in the northern, southern and eastern parts of the study area to about 40 m depth. Similarly, [21], investigated leachate contamination at a major open dumpsite in Eket, Southern Nigeria, using VES and ERT methods, constrained by well lithological information. Dar-Zarrouk indices and electrical reflection co-efficient indicated that the highly heterogeneous region had moderate aquifer protective capacity and moderate aquifer potentiality. They recommended sanitary landfills, phyto-remediation, impermeable liners to diminish the rate of leachate percolation in the area. [2] investigated leachate infiltration and its potential influence on groundwater resources at Ojoou, Olayanju's dumpsite, southwestern Nigeria, combining geo-resistivity and natural electric field (NEF) methods. Five dipole-dipole and five NEF measurements were obtained using the Omega resistivity meters and PQWT-150 equipment respectively. Results revealed that the conductive medium within the study area is saturated with leachate, which suggests that very large portion of the study area has been contaminated by leachate. They concluded that the groundwater quality in the area is at risk of contamination with the continuous infiltration of leachate.

AIM AND OBJECTIVES OF THE STUDY

The aim of this study is to conduct the aquifer vulnerability assessment around a major dumpsite in Goshen City in Nasarawa State, using integrated geophysical methods.
The specific objectives of this study are to:

Determine the aquifer vulnerability capacities of the layers underlying the study areas;
Delineate areas of contaminant plume and assess their extent of migration into the subsurface;
Determine the hydraulic characteristics and groundwater yield of the study areas;
Determine the depth-to-bedrock and factors controlling groundwater occurrence within the study areas; and
To provide efficient policy formulation guide on waste disposal design.

2.1.1 SITE LOCATION AND GEOLOGY

The Goshen dumpsite and its control centre are situated between latitude ($8^0 56^{'} 8.0874^{''}$N and $8^0 56^{'} 8.232^{''}$ N) and longitude ($7^0 40^{'} 52.1178^{''}$ E and $7^0 40^{'} 35.241^{''}$ E) within Aso Kadape ward in the Nyanya Gwandara general area, Karu LGA of Nasarawa State. It is underlain by the Basement Complex Rocks of Nigeria, which consists of the migmatite gneisses, the schist belts, the Older Granites suite comprising mainly different varieties of granitic rocks, including charnockites (hypersthene granites), syenites, as well as minor gabbroic and dioritic rocks, and the undeformed

acid and basic dykes [5]. These rocks have undergone polycyclic deformation, thereby causing the formation of both micro and macro structures. The general structures include joints, foliations, and faults [5]. They generally have NNE-SSW trending gneissose foliations with few ENE-WSW and NNW-SSE trends and dip values which vary from as low as 6° to as high as 60° in the S-E directions [15, 5, 20]. The area is characterized by highlands and lowlands with least elevation values lower than 260 m (above sea level) in the area around the S-E, close to River Uke flow path. The highest relief point rises to heights of 410 m (asl) around S-W, which is an intrusive outcrop. The drainage pattern in the area is dendritic and this reflects a resistance to erosion by the underlying rock units. The study areas are influenced by two major climatic conditions, the rainy seasons begin in April and peaks in August through October and the dry season from February to early-mid April. The harmattan (dry and dusty wind) experienced from November - January also characterises the dry season. The mean annual rainfall is 145.66 mm per annum [4].

Plate 1: Goshen Dumpsite and its control centre (Source: Google Earth)

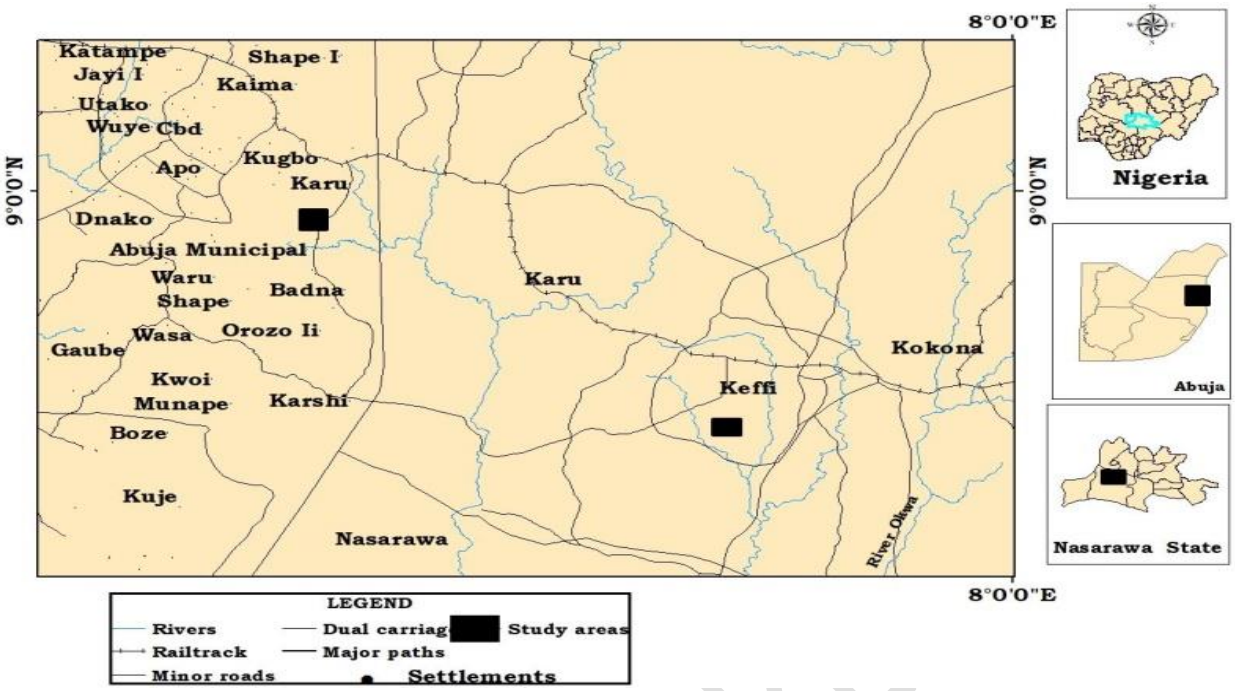

Figure 1: Location map of the study areas [22]

Figure 2: Topographic map of the study area [22]

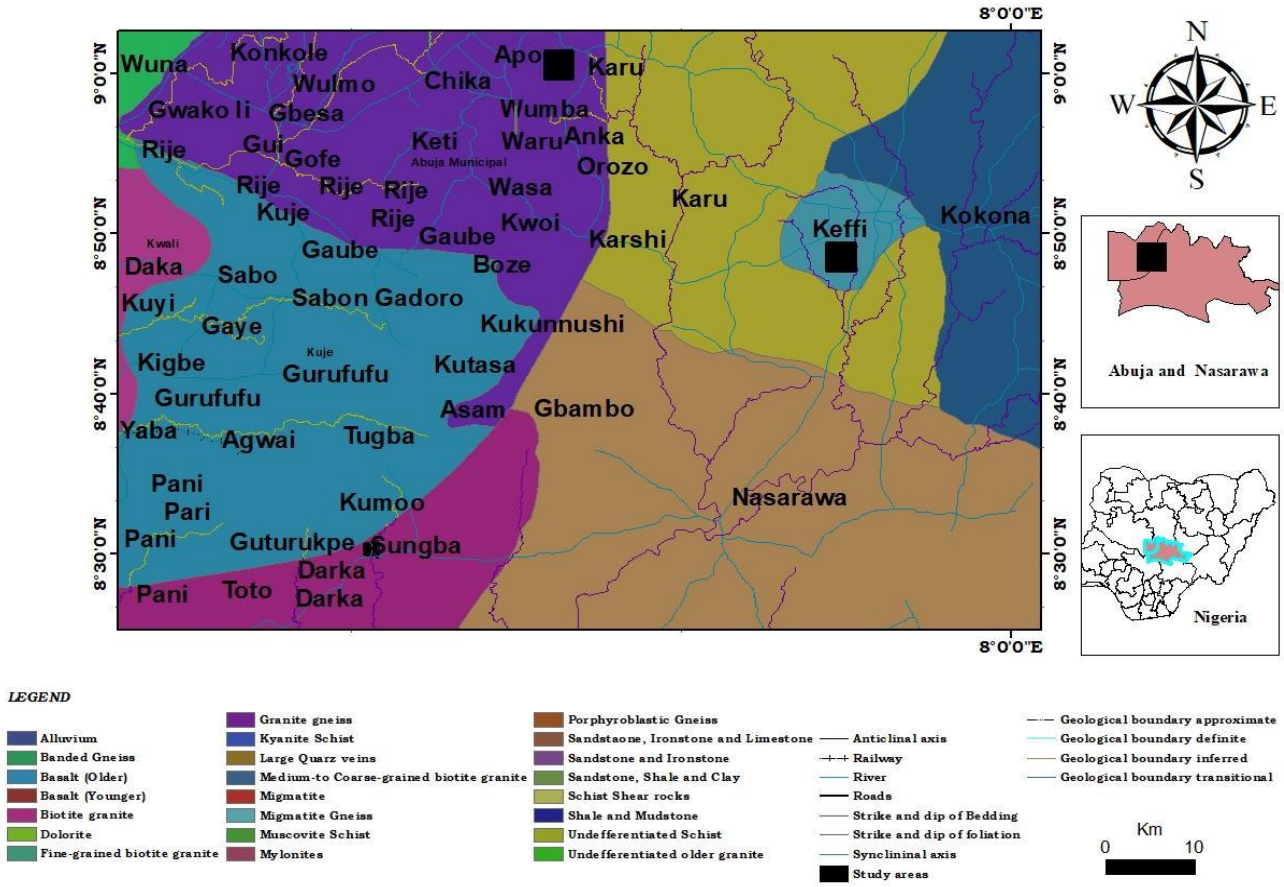

Figure 3: Geological map of the study areas [10]

3.1 MATERIALS AND METHODS

Fourteen VES points were probed within the dumpsite, while one transverse was created at the control site using the Schlumberger array configuration with maximum current electrode spacing (AB/2) of 170 m at each point using the Ohmega Allied resistivity meter to determine the electrical resistivities and depths of the subsurface layers. Borehole logs were used to correlate the VES cross-sections. On the other hand, two 2-D ERT profiles were created within the dumpsite, while one 2-D ERT transverse was created at the control centre with the resistivity metre using the wenner array configuration along the same transverses. The resistivity survey profiles were laid radially from the site into the community with the length of the profile depending on the proximity of the dumpsite to the community. The profile lengths ranged from 0 to 120 m at constant electrode spacing of 5 to 25 m. The 2-D inverse resistivity models of the subsurface were obtained from the input resistivity data using the inversion code of RES2DINV.

3.1 Estimation of Aquifer Protective Capacity (APC)

The estimation of the aquifer protective capacity can be based on the values of the longitudinal unit conductance (S) of the overburden rock units using the longitudinal conductance/protective capacity rating [3].

The total transverse resistance R is given by:

$$R=\sum_{i=1}^{n} h_i \rho_i \quad (1)$$

For a horizontal, homogeneous, and isotropic medium:

$$\rho=\frac{(R_1-R_2)}{(h_1-h_2)} \quad (2)$$

The total longitudinal conductance S is:

$$S=\sum_{i=1}^{n} \frac{h_i}{\rho_i} \quad (3)$$

where h_i and ρ_i are the thickness and resistivity of the i^{th} layer in the section, respectively.

The longitudinal layer conductance Si can also be expressed by:

$$S=\sigma_i h_i \quad (4)$$

where h_i is the layer thickness and ρ_i is layer resistivity, while the number of layers from the surface to the top of aquifer varies from i = 1 to n (Table 1):

Table 1: Modified longitudinal conductance/protective capacity rating [12]

Longitudinal Conductance (mhos)	Protective Capacity Rating
>10	Excellent
5-10	Very Good
0.8-4.9	Good
0.2-0.79	Moderate
0.1-0.19	Weak
<0.1	Poor

3.1.1 VLF-EM Data Acquisition

A total of nine VLF-EM profiles were created within the dumpsites, while one VLF-EM profile was established at the control centre. The VLF-EM data were collected with the aid of GEM Portable EM receiver systems at the frequency range of 15.1 – 24.0 kHz. It was not possible to have a perfectly regular grid of data points due to irregular topography around the dumpsites. Parts of the area investigated had already been surveyed using the ERT, VES and SP methods. The VLF profiles were used to determine contaminant paths with stations distance 5 m apart. The in-phase profiles revealed positive peaks of different intensities and sharpness, suggesting the presence of shallow and deep conductors. The Fraser filter transformed the zero-crossing points into peaks enhancing the signals of the conductive structures. The centre of the anomalous structure fall directly under the peak of the Fraser filtered data. The plotted cross-sections indicated the Fraser filtered data (real or in-phase components) and the measured values.

3.1.2 The VLF-EM Diagnostics

In-phase (abbreviation IP) and Quadrature (abbreviation Quad) are the two most important field measurements of the VLF method and can be expressed as the normalized real and quadrature components of the vertical magnetic field:

$$inphase = \frac{real(H_z)}{\sqrt{(H_x^2 + H_y^2)}} \quad 5$$

$$Quad = \frac{imag(H_z)}{\sqrt{(H_x^2 + H_y^x}} \quad 6$$

3.2 Theory and Principles of Self-Potential

The self-potential method is a passive geophysical method involving the measurement of the electric potential at a set of measurement points called self-potential stations [17]. The sampled electrical potential (or electrical field) can be used (inverted) to determine the causative source of

current in the ground and obtain important information regarding groundwater flow, hydro-mechanical and geo-chemical disturbances.The general equation for coupled flows [14] can be written as:

$$J_i = \sum_j L_{ij} X_j \qquad 7$$

where the fluxes J_i (of charges, matter, heat, etc) are related to the various forces X_j (gradients of electrical potential, pressure, temperature, etc) through the coupling coefficients L_{ij} (‘‘phenomenological coefficients’’ [7] or ‘‘conductivities’’ [19].

3.3 Self-Potential (SP) Data Acquisition

Nine SP profiles were established within the dumpsites, while one was established at the control centre. Two non-polarizing electrodes constructed by the solutions inserted into saturated copper sulphate with copper electrode in the middle and the Ohmega (Allied Geophyics) model resistivity metre used for the SP data collection. Readings were taken with one electrode fixed at a base station and a second one, the mobile ‘field’ electrode moved along every sampled profile around the survey area. Reading stations were distributed at regular intervals of 5 m along linear profiles with maximum electrode spacing of 165 m. The SP data interpretation is mainly qualitative (profile, map) [9].

4.1 RESULTS AND DISCUSSIONS

The summary of results for the fifteen (15) VES points conducted within the Goshen Dumpsite and its control centre, indicating the No. of layers, Curve Types, resistivity values (Ω.m), thicknesses (m), depth (m) and delineated lithological units are presented in Table 2:

Table 2: Vertical Electrical Sounding data for VES stations 1-15 (Goshen)

VES	No. of Layer (s)	Curve Type (s)	Res. (Ω.m)	Thickness (m)	Depth (m)	Lithological Units
1	4	H	283.1	0.3	0.3	Topsoil (lateritic)
			7.0	1.9	2.2	Sandy- clay
			46651.3	175.8	178	Fresh Basement
			5631.8	-	-	Partial fresh Basement
2	5	HA	1857.9	0.9	0.9	Topsoil
			19.2	2.7	3.7	Sandy-Clay
			95.1	2.6	6.3	Weathered/Fractured basement
			18068	38.8	45	Partial fresh Basement
			30439.5	-	-	Fresh Basement
3	5	HK	1939.5	1.7	1.7	Topsoil
			35.3	2.9	4.6	Weathered layer (Saturated silt clay)
			254.9	13.5	18.1	Fractured basement
			21351.7	137.1	155.1	Partial fresh Basement
			5501.1	-	-	Fresh Basement

4	4	HK	2775.8	1	1	Topsoil
			17.6	2.7	3.6	Sandy-Clay
			1050.9	4.4	8	Partial fresh Basement
			37985.6	-	-	Fresh Basement
5	4	HA	3044.1	0.3	0.3	Topsoil
			16.6	5.2	5.5	Weathered basement
			2530.7	13.1	18.6	Partial fresh Basement
			20170.6	-	-	Fresh Basement
6	5	QA	96.6	1.2	1.2	Topsoil
			14.8	3.2	4.4	Weathered basement
			1.6	5.1	9.6	Sandy-leachate
			177.3	10.8	20.3	Weathered basement
			3278.4	-	-	Fresh Basement
7	5	H	6019.8	0.8	0.8	Topsoil
			6.4	7.7	8.5	Sandy-leachate
			77.5	15.3	23.8	Weathered basement
			3.3	99.6	123.4	Leachate
			11.3	-	-	Sand, Leachate
8	5	HA	217.9	1.6	1.6	Topsoil (Lateritic)
			3.9	2	3.7	Sandy-Leachate
			30.3	2	5.7	Weathered basement
			9178.4	76	81.7	Fresh Basement
			5901.5	-	-	Partial fresh Basement
9	4	HK	128.5	1	1	Topsoil
			28.3	4.4	5.4	Clayey-sand
			26784.7	159.4	164.8	Fresh Basement
			3950.9	-	-	Partial fresh Basement
10		HA	91.2	1.3	1.3	Topsoil
			20.8	2.3	3.6	Saturated sandy soil
			389.2	2.9	6.5	Fractured basement
			44739.6	-	-	Fresh Basement
11		KH	223.6	1.4	1.4	Topsoil
			295.9	2.5	3.9	Weathered/Fractured layer
			140.8	6.2	10.1	Weathered basement
			614428	-	-	Fresh Basement
12		HK	371.8	0.5	0.5	Topsoil
			12.4	1.3	1.8	Sandy clay
			366	1.6	3.4	Fractured basement
			100000	-	-	Fresh Basement
13		KH	141.8	0.8	0.8	Topsoil
			517.4	1.9	2.7	Weathered/Fractured basement
			82.1	5.2	7.8	Weathered

			81,656.2	-	-	Fresh Basement
14		HK	117	1.5	1.5	Topsoil
			13.8	1.9	3.5	Sandy-clay
			1585.9	5.1	8.5	Fresh basement
			37615	-	-	Partial fresh Basement
15	3	A	59.3	3	3	Topsoil
			42612.2	20	23	Partial fresh Basement
			100000	-	-	Fresh Basement

4.1.1 Estimated Aquifer Parameters of the surveyed area (Goshen)

The primary aquifer parameters (resistivity and thickness) are determined from Table 2 and used to estimate the geo-hydraulic parameters. The summary of the Daz-Zarrouk parameters estimated for the weathered aquifers showing the VES points, resistivity values ρ (Ω.m), Aquifer thicknesses h (m), Electrical conductivity σ ($\Omega.m^{-1}$), Longitudinal Conductance S (mhos), Transverse Resistance T_R ($\Omega.m^{-2}$), Hydraulic conductivity K (m/day), Transmissivity T (m^2/day), Quantity of water and porosity ϕ (%) are presented in Tables 3 and 4:

Table 3: The summary of Dar-Zarrouk parameters and electrical conductivity K (m/day) estimated for the weathered aquifers in the study area (Goshen)

VES	**ρ (Ω.m)**	**Thickness (h/m)**	**$\sigma = 1/\rho$ ($\Omega.m^{-1}$)**	**$S = \sigma h$ (mhos)**	**$T_R = h\rho$ ($\Omega.m^{-2}$)**	**K (m/day)**
1	7.0	1.9	0.1429	0.2714	13.3	62.908
2	95.1	2.6	0.0105	0.0273	247.1	5.517
3	254.9	13.5	0.0039	0.0529	3441.1	2.199
4	17.6	2.7	0.0568	0.1534	47.52	26.618
5	16.6	5.2	0.0602	0.3132	86.32	28.111
6	177.3	10.8	0.0056	0.0609	1914.84	3.086
7	3.3	99.6	0.3030	30.1818	328.68	126.870
8	30.3	2.0	0.0330	0.0660	60.6	16.036
9	28.3	4.4	0.0353	0.1555	124.52	17.090
10	389.2	2.9	0.0026	0.0075	1128.68	1.482
11	140.8	6.2	0.0071	0.0440	872.96	3.826
12	366	1.6	0.0027	0.0044	585.6	1.569
13	82.1	5.2	0.0120	0.0630	426.92	6.328
14	13.8	1.9	0.0724	0.1380	26.22	33.398
15	42612	20	2.4E-05	0.0004	852244	0.0185

Table 4: The summary of aquifer transmissivity (T), quantity of water Q and porosity ϕ (%) estimated for the weathered aquifers in the study area (Goshen)

VES	T = kh (m^2/day)	Quantity Q = (kσ)	Porosity ϕ (%)
1	119.525	8.9868	44.14
2	14.35	0.06	33.19
3	29.6918	0.0086	29.05
4	71.870	1.5124	40.27
5	146.179	1.6934	40.51
6	33.3271	0.0174	30.57
7	12636.0	38.444	47.29
8	32.0725	0.5293	37.99
9	75.20	0.604	38.27
10	4.2978	0.0038	27.27
11	23.722	0.0272	31.54
12	2.511	0.0043	27.53
13	32.907	0.077	33.80
14	63.456	2.420	41.29
15	0.3711	4.4E-07	7.56

4.1.2 Results of computer modeled curve for fifteen (15) VES points (Goshen)

The results of the computer modeled curves for the fifteen (15) VES points conducted within Goshen dumpsite and its control centre are shown in Figures 11 to 25:

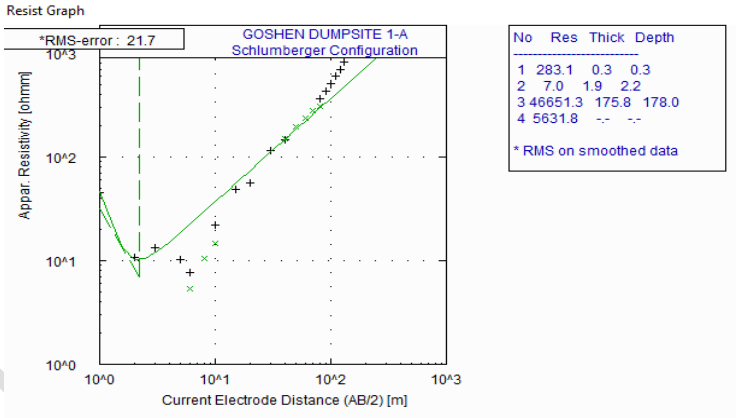

Figure 4: Results of computer modeled curve for VES 1

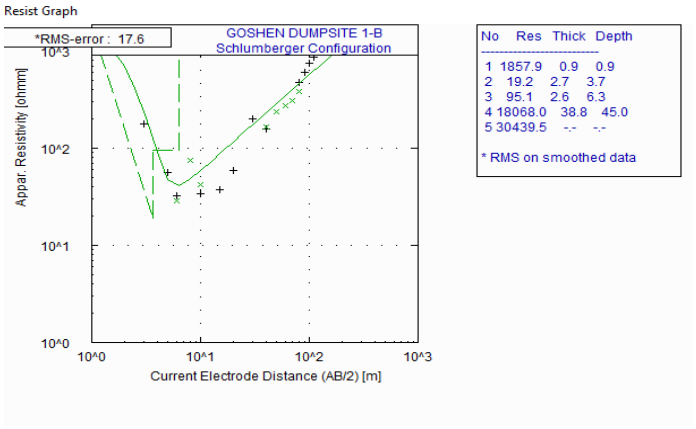

Figure 5: Results of computer modeled curve for VES 2

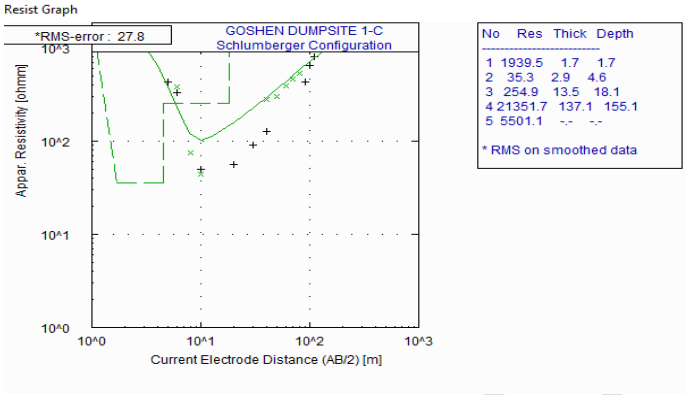

Figure 6: Results of computer modeled curve for VES 3

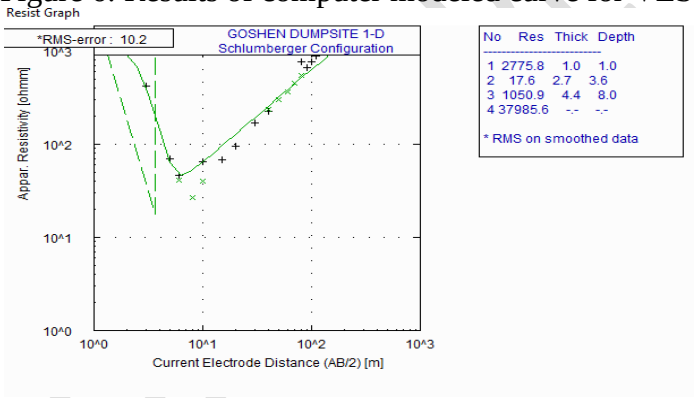

Figure 7: Results of computer modeled curve for VES 4

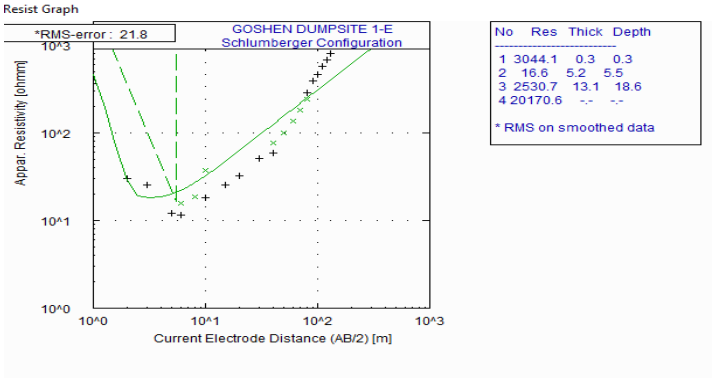

Figure 8: Results of computer modeled curve for VES 5

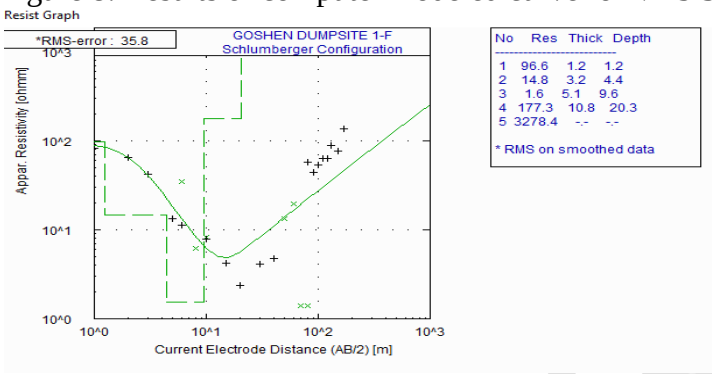

Figure 9: Results of computer modeled curve for VES 6

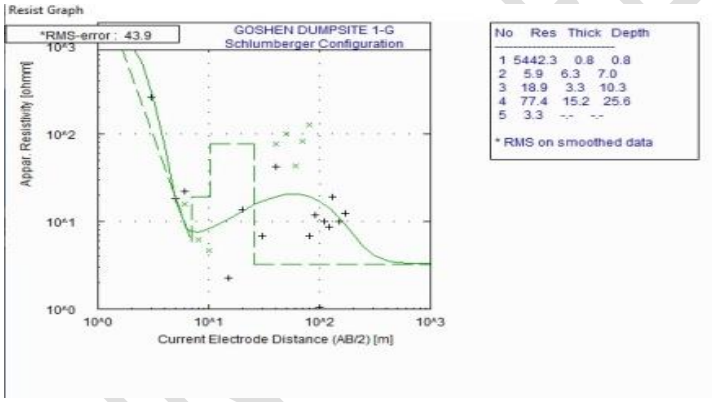

Figure 10: Results of computer modeled curve for VES 7

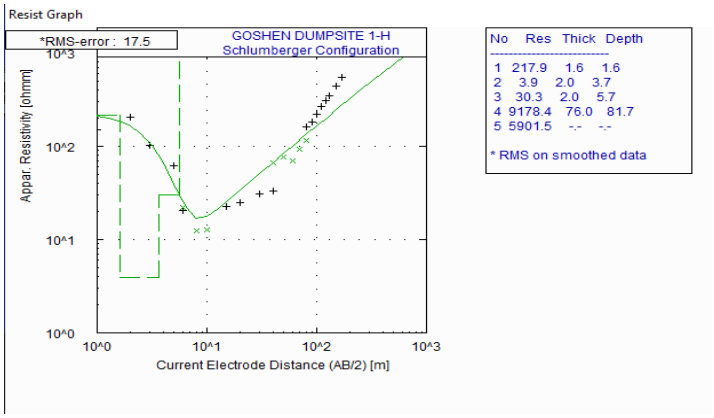

Figure 11: Results of computer modeled curve for VES 8

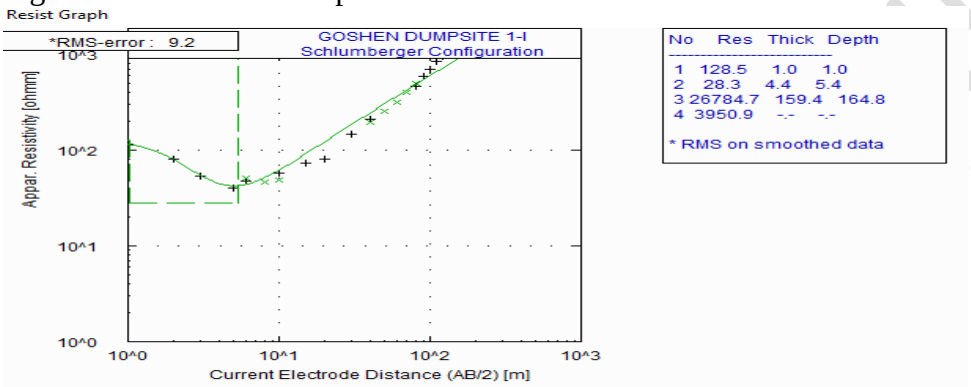

Figure 12: Results of computer modeled curve for VES 9

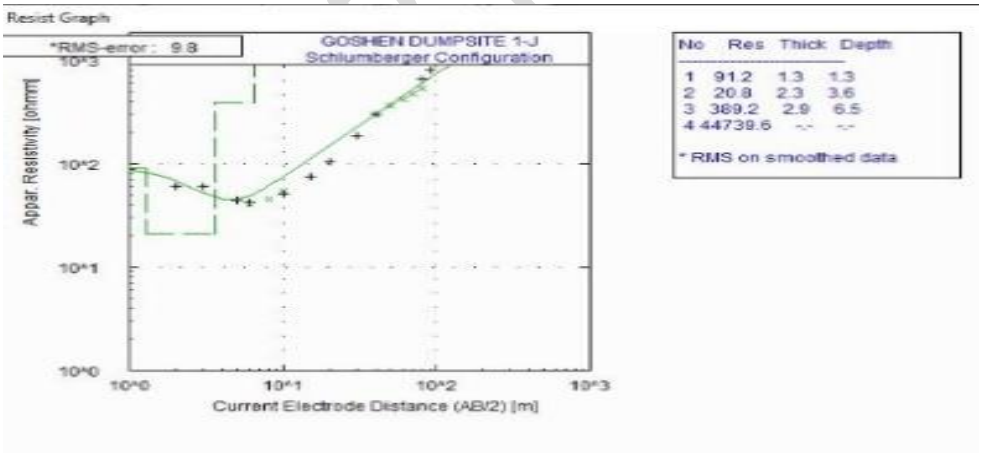

Figure 13: Results of computer modeled curve for VES 10

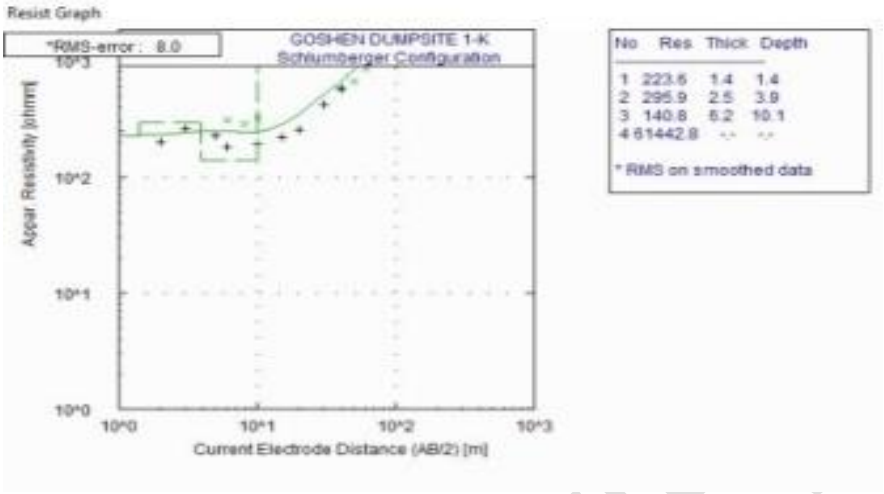

Figure 14: Results of computer modeled curve for VES 11

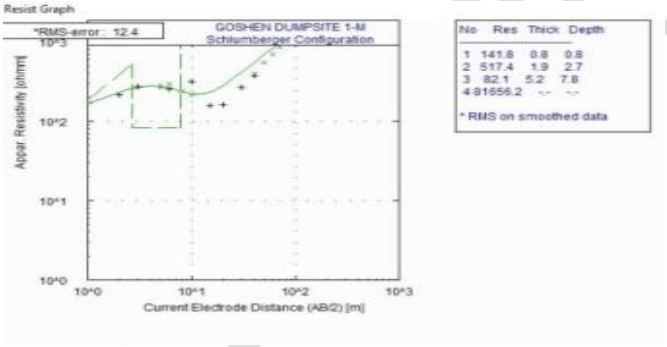

Figure 15: Results of computer modeled curve for VES 12

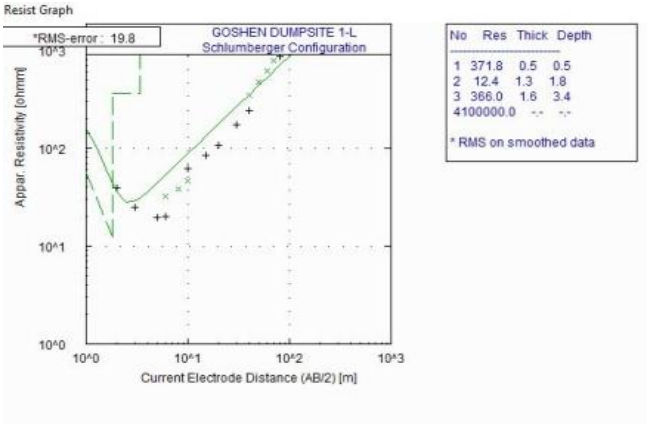

Figure 16: Results of computer modeled curve for VES 13

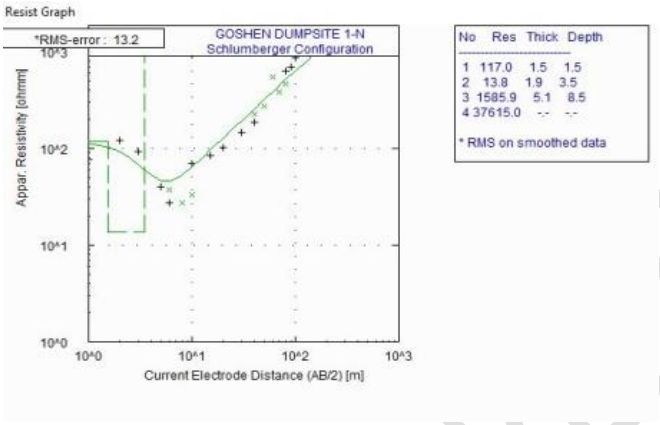

Figure 17: Results of computer modeled curve for VES 14

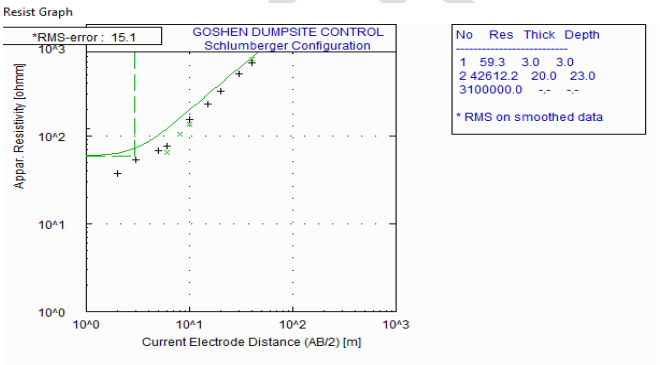

Figure 18: Results of computer modeled curve for VES 15 (Control)

4.1.3 Correlation of Borehole log with VES

The correlation of borehole lithological logs BH (D) and BH (C) [16] with resistivity sounding (VES) results for VES 1-6 and for VES 7 – 15 for the study area are shown in Figures 19 and 20:

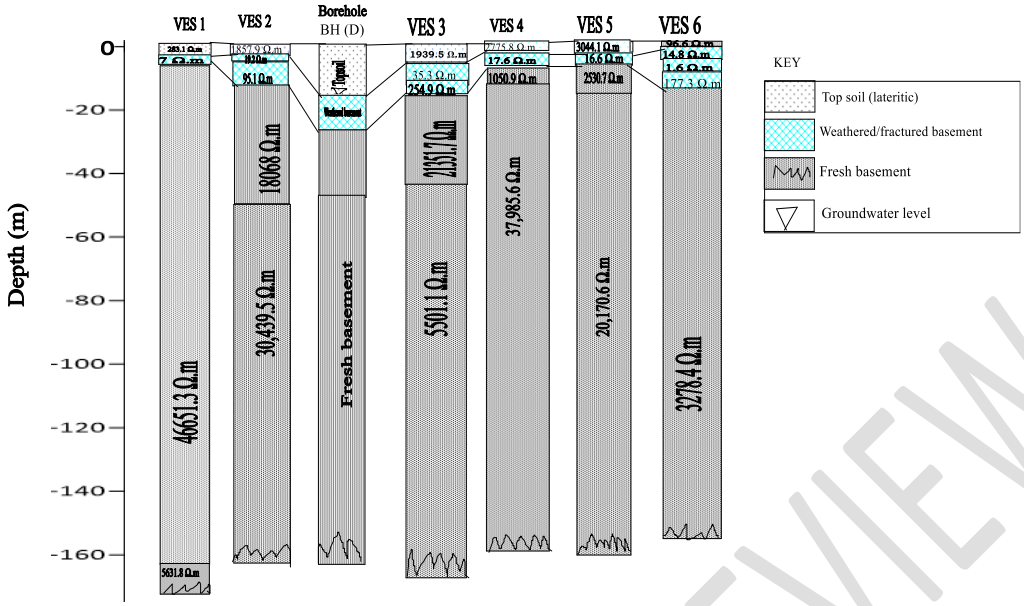

Figure 19: Correlation of resistivity sounding (VES) results with borehole lithological logs in the study area

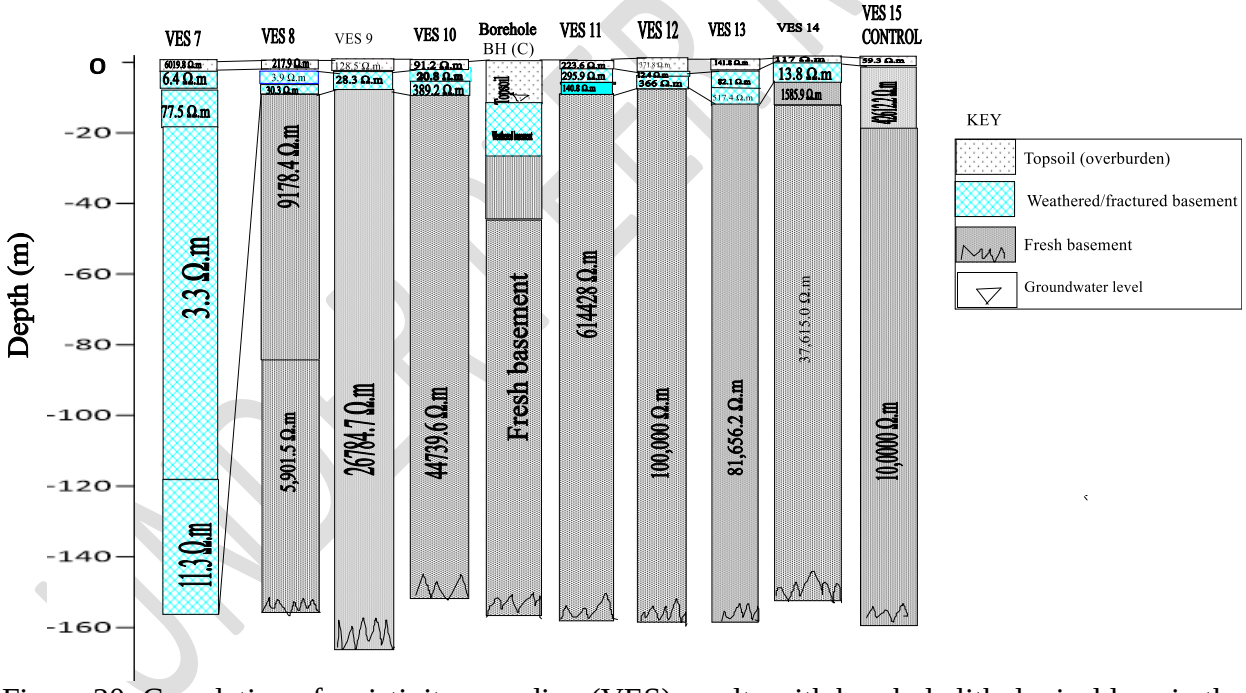

Figure 20: Correlation of resistivity sounding (VES) results with borehole lithological logs in the study area

4.1.4 Discussion

The measured apparent resistivity curves and results of the 1-D inversion that correlate well with the measured values are displayed in the corresponding resistivity-depth profiles in Figures 19 and 20. The VES data revealed four to five discrete geo-electric layers, such as Topsoil consisting of

lateritic soil; second layer - interpreted as clayey sand; third layer - inferred as weathered/fractured; the fourth and fifth layers - interpreted as fresh bedrock. The Curve Types identified from the model include: HA (26.7 %), HK (26.7 %), H (13.3 %), KH (13.3 %) QA (6.7 %), while the A (6.7 %) type curve was identified at the Control Centre.

4.1.5 The Topsoil

Resistivity values for Topsoil ranges from (96 to 1857.9 Ω.m) with corresponding depths ranging from (0.3 to 3 m) and thicknesses (0.3 to 3 m). This is suggestive of three zones: the belt of the soil water at the top, the intermediate vadose zone, and the capillary fringe at the bottom which acts as the passage for the flow of surface water to the fractured layer known as the zone of aeration.

4.1.6 The Second layer

The resistivity values of the second layer ranges from (3.9 to 35 Ω.m) with corresponding depths of (2.2 to 8.5 m) and thicknesses ranging from (1.9 to 7.7 m). This layer is mostly composed of weathered to fractured basement, clay, leachate and consolidated sandstones. The varying levels of compaction in the clayed sand may account for the contrasting resistivity values in this layer.

4.1.7 The third layer

The resistivity values of the third layer ranges from (1.6 to 2530.7 Ω.m) with corresponding depths ranging from (3.4 to 178 m) and thicknesses (1.6 to 159.4 m). This is likely composed of clay, weathered/fractured basement to fresh basement. The increase in resistivity values in basement rocks is a function of lower fracture density or lower levels of weathering as seen in the boundary between layers 3 and 4, close to the fresh basement, with the resistivity values of the fourth layer ranging from (3,950.9 to 26784.7 Ω.m), with corresponding depths ranging from (20.3 to 155.1 m) and thicknesses (10.8 to 137.1 m). The resistivity values tend to increase towards the boundary between layers 3 and 4 attributed to the increase in grain size.

4.1.8 The conductive layers

Conductive layers with resistivity values lesser than 6.83 (Ω.m) were delineated as leachate infiltrated and soil-contaminated zones which has spread along transverses 1, 6, 7 and 8 to a maximum depth of about 99.6 m at an average depth of 27.15 m.

4.1.9 Estimated Aquifer Protective Capacity (APC) for Goshen study area

The calculated Longitudinal Conductance S (mhos) (Tables 3 and 4) revealed that the aquifer protective capacity of the study area is rated as poor to excellent with only VES 7 (30.18 S) representing (6.7%) rated as excellent; two (2) VES points; VES 1 (0.27 S) and VES 5 (0.31 S) representing (13.3 %) rated as moderate, VES points, VES 4 (0.153 S), VES 9 (0.155 S), VES 14 (0.14 S) representing (20 %) rated as weak, while, VES 8 (0.066 S), VES 6 (0.061 S), VES 3 (0.053 S), VES 11 (0.044 S), VES 2 (0.027 S), VES 10 (0.0075 S), VES 13 (0.0063 S), VES 12 (0.0044 S), VES 15 (0.00046 S), representing 60 % of the sounding points, show poor protective capacity rating. The combined rating of VES points indicating weak to poor protective capacity (80 %), suggests that the study area is not suitable for the establishment of a dumpsite, as there is no sufficient impervious clay seal to protect groundwater resources against leachate infiltration.

4.2 Results of the Self-Potential (SP) survey conducted in the study area

The results of the ten (10) SP profiles conducted in the study area are shown in Table 5:

Table 5: Summerised results from Self-Potential (SP) survey in the study area

Distance X (m)	SP (mV) 1	SP (mV) 2	SP (mV) 3	SP (mV) 4	SP (mV) 5	SP (mV) 6	SP (mV) 7	SP (mV) 8	SP (mV) 9	SP (mV) 10 (Control)
0	-99	-44.3	8.3	-13.5	-63.3	151	-50	-48	-35	92
5	-27	-80	-28	-14.7	-91.2	143	-133	-24	81	154
10	1.8	-26	-5.3	-43.4	-69.3	127	-34	11.4	2.7	144
15	39.5	-65.8	-32	-11.1	-143	67	-33	-76	111	84
20	6.31	-29.7	30	-14.1	-101	33	-59	-8.8	174	150
25	11	-113	49	-14	-49.4	14	-23	-34	86	33
30	-22	-92	92	-10.8	-70.3	23	-39	-39	-10	163
35	53.1	-47.3	93	72.1	-71.5	-8.3	-74	-33	18	108
40	39.6	-30.1	49	56.7	-75.4	37	-89	-59	-9	137
45	8.59	57.6	48	37.7	-86.9	138	-578	-35	22	122
50	80.1	8.14	97	88.7	-78.5	72	-231	-38	-32	136
55	8.65	-16.8	50	102.	-84.2	71	-78	-91	32	123
60	18.5	25.6	9.6	70.5	-77.5	133	-146	-59	-23	137
65	15	24.18	40	105.5	-95.7	28	0.7	-5.4	-26	171
70	9.59	-78.9	8.8	99.6	-90.8	57	-105	-11	4.6	208
75	56.2	26.53	100	30.63	-128	41	-57	-42	52	247
80	-66	18.13	55	73.98	-49.6	57	-39	3.34	-47	170
85	-55	11.98	4.4	226.2	-47.8	9.7	-69	15	-21	239
90	-59	10.75	32	63.94	-68.9	59	-85	-7	45	262
95	9.37	28.38	72	55.74	-38.3	140	-26	80.3	18	165
100	-28	43.85	41	-0.44	102.4	124	-113	49.6	-41	227
105	52.3	58.2	34	72.54	-93.5	83	-11	28.9	15	203
110	73	40.37	84	130.1	-32.2	144	-29	27.7	-85	206
115	-3.8	-12.8	58	159.3	-56.4	119	-41	27.2	30	239
120	-4	-4.14	-35	51.64	-44.7	152	-105	3.98	2.4	206
125	41.8	11.27	-5.3	69.4	-43.7	-1.2	-121	28.6	6.9	159
130	-5.1	-1.46	23	94.88	-67.8	109	-96	-69	-6	211
135	14.1	26.64	76	63.32	-88.3	154	-67	-114	-24	143
140	-14	13.42	17	95.91	-34	144	-65	-18	-1	202
145	-86	18.54	-3.3	97.55	-96.3	113	-42	-109	27	181
150	-18	50.62	-2.4	101.2	-77.5	29	26	-109	66	225
155	29.7	-24.8	-	138.3	-34.8	-	-	-102	9.6	171
160	-	-	-	-	-	-	-	-87	-	-
165	-	-	-	-	-	-	-	-22	-	-

4.2.1 Discussion

The following cross-sections correlates the Self-Potential (mV) profiles, SP contours and 3-D SP plots, VES logs and 2-D ERT geo-electric sections to compare leachate contaminated areas along the survey lines (Figures 21 – 30):

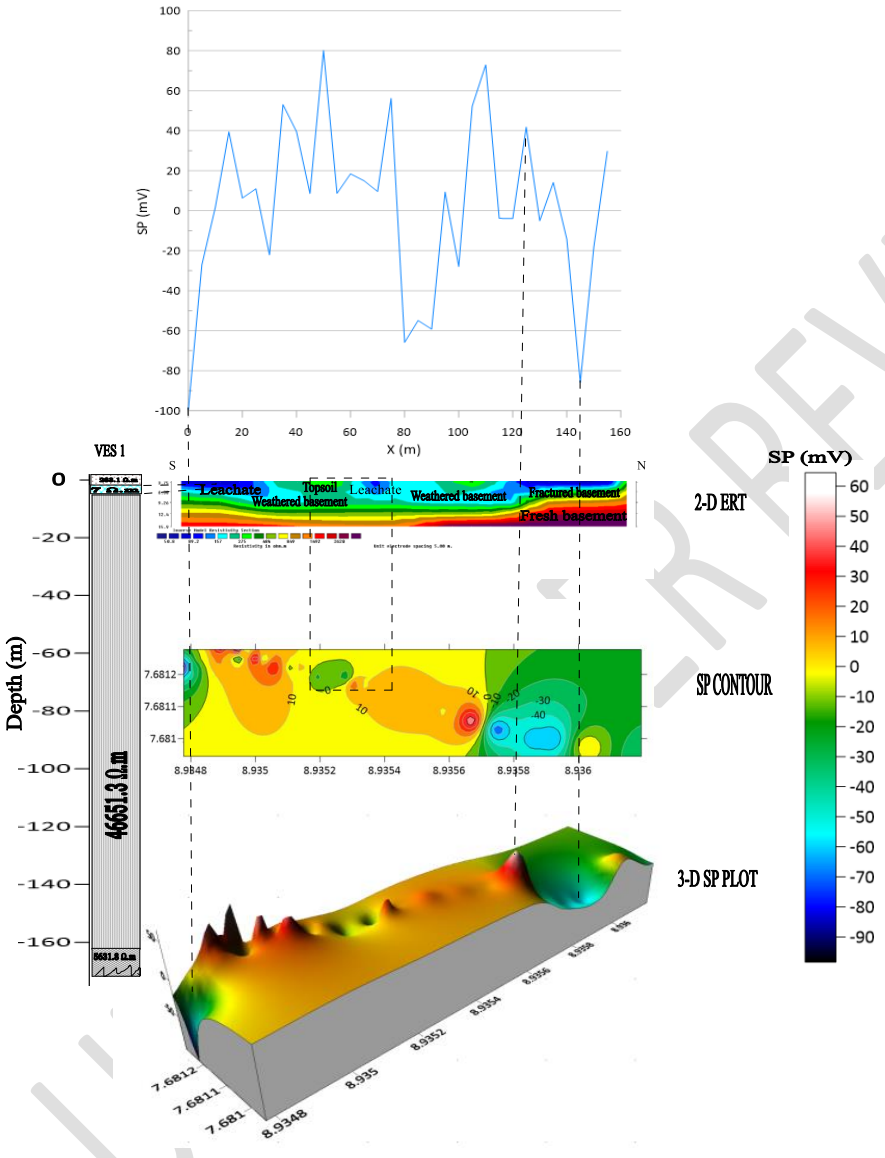

Figure 21: Cross-section correlating the 2-D ERT geo-electric section, VES transverse, Self-Potential in (mV) signal, SP contour and 3-D SP plot along profile 1

4.2.2 Discussion

This cross-section (Figure 21) correlates the 2-D ERT geo-electric section, SP profile, SP contours, 3-D SP plot, and VES Log, along profile 1. Starting from the southern flank in the 2-D ERT line are materials with low resistivity values ranging from 50.8 to 53 (Ω.m) extending to depths of 1.25 to 6.38 m between (0 to 20 m). This is suggestive of weathered layer infiltrated by leachate

contaminants. To the northern flank, spanning between 50 to 90 m, are materials with similar resistivity values ranging from (49 to 51 Ω.m). This was also interpreted as sandy weathered/fractured zone hosting conductive materials. The dominant negative SP distribution patterns ranging from (-80 to -30 mV) situated between (0 to 10 m), and the SP values ranging from (-90 to -40 mV) situated between (120 and 140 m) are attributed to differences in mobility and concentration of ions emanating from percolated organic and inorganic materials from the dumpsite. The materials with low resistivity values of (7 Ω.m) covering depths of 2.2 m along the VES log, suggests accumulation of leachate which correlates with the SP and 2-D ERT results.

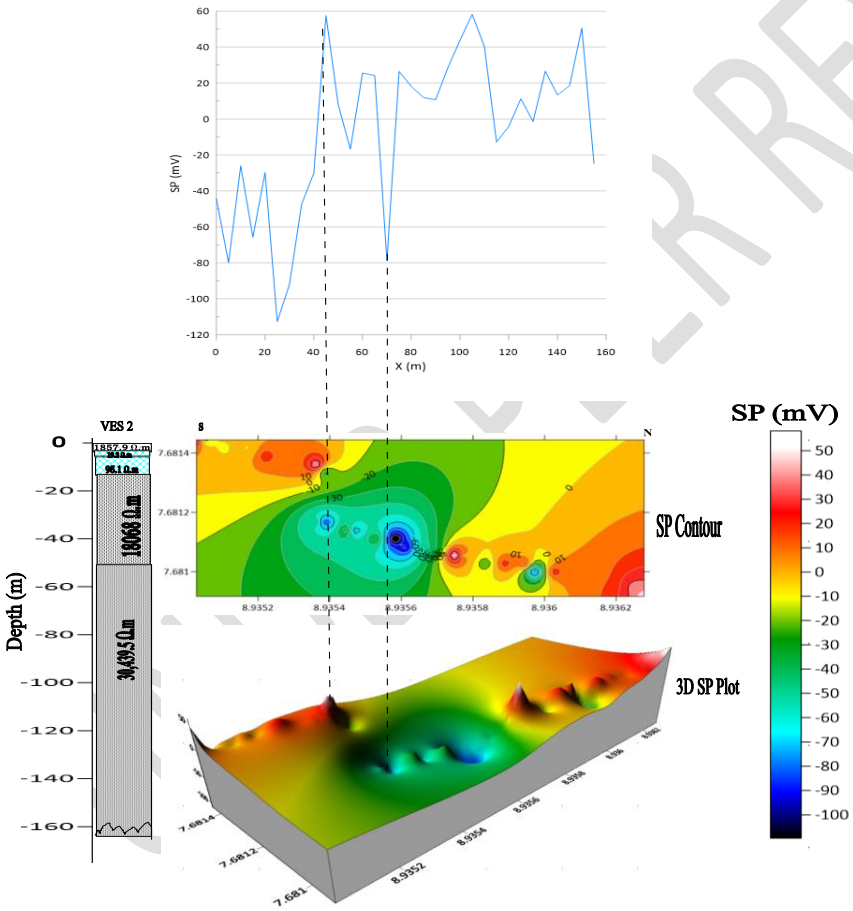

Figure 22: Cross-section correlating the VES transverse, Self-Potential in (mV) signal, SP contours and 3-D SP plot along Profile 2

4.2.3 Discussion

This cross-section (Figure 22) correlates the SP (in mV) profile, the SP contours, the 3-D SP plot and the VES log for profile 2. Self-Potential profile shows variation of positive and negative SP values ranging from (-100 to 50 mV). The negative SP values peaked between (-90 to -30 mV) at the central point of the contour map situated between (60 to 100 m) interpreted as leachate contaminants flowing in the S–N direction. This correlated by presence of objects with low resistivity values of (19.2 Ω.m) observed along the VES log interpreted as leachate infiltrated zone.

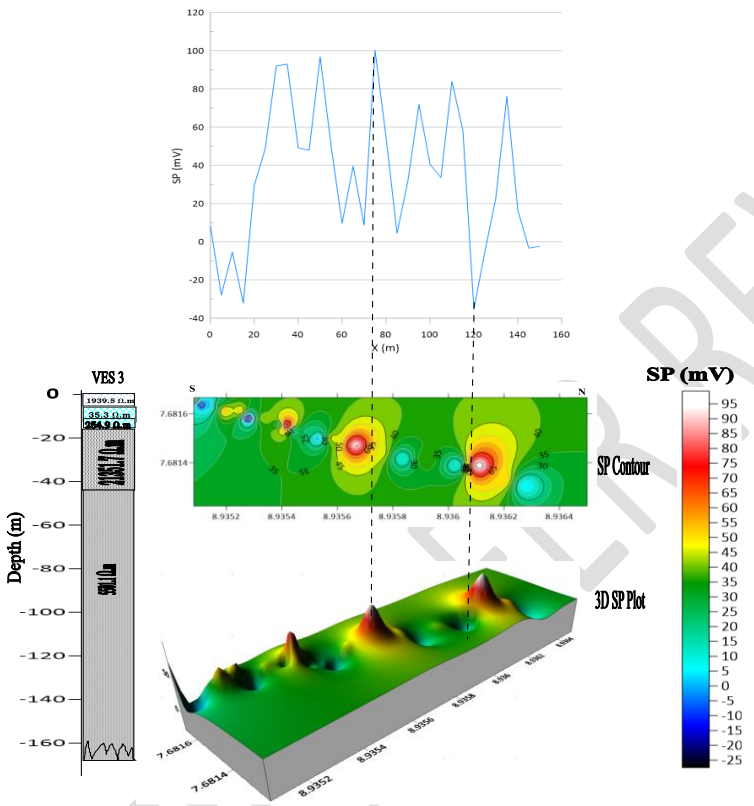

Figure 23: Cross-section correlating the VES transverse, Self-Potential in (mV) signal, SP contours and 3-D SP plot along Profile 3

4.2.4 Discussion

This cross-section (Figure 23) correlates the VES Log, 2-D SP contours, the 3-D SP plot and SP (in mV) signals for profile 3 running in the South – North direction. The self-potential profile in this cross-section shows variation of positive and negative SP values ranging from (-25 to 95 mV). However, the material with dominant negative SP values ranging from (-25 to -5 mV) which peaked between (0 to 20 m) and (110 and 120 m) is attributed to electrochemical reaction from groundwater flowing in the S-N direction. This result was correlated by materials with resistivity values of (35.3 Ω.m) occurring along the VES transverse, suggestive of groundwater occurrence. The positive SP anomaly ranging from (40 to 95 mV) at points 55m and 75 m along the profile is characteristic of quartz veins.

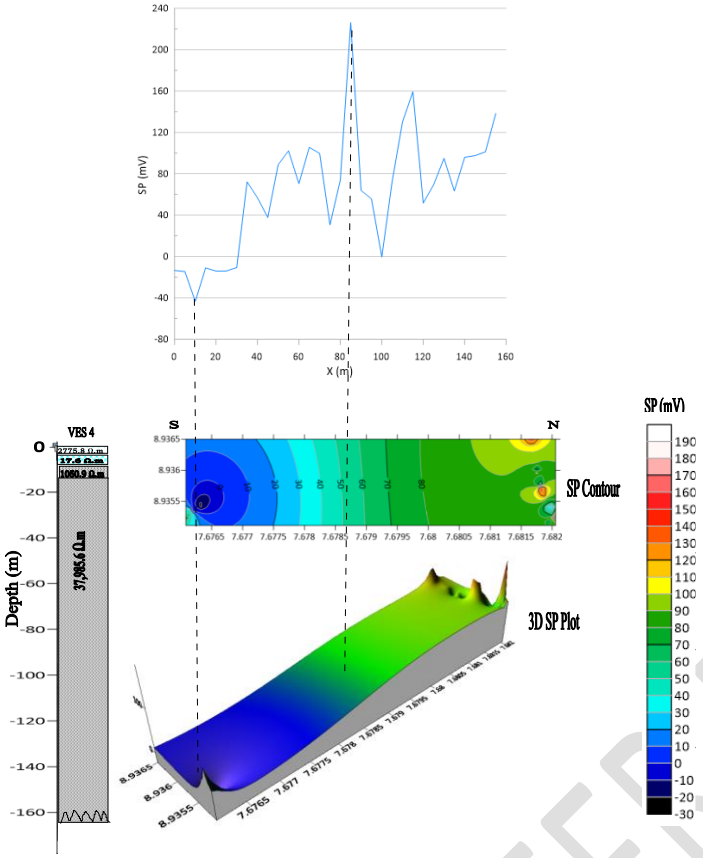

Figure 24: Cross-section correlating the VES transverse, Self-Potential in (mV) signal, SP contours and 3-D SP plot along Profile 4

4.2.5 Discussion

This cross-section (Figure 24) correlates the VES Log, 2-D SP contours, the 3-D SP plot and SP (in mV) signals for profile 4. It indicates variation of positive and negative SP values ranging from (-41 to 220 mV). From the southern flank, (0 to 40 m) are objects dominated by (-30 to -10 mV) negative SP values attributed to electro-kinetic processes occasioned by leachate plume from the dumpsite running in the North – South direction. This was correlated by VES log 4 indicating materials with the low resistivity values of (17.6 Ω.m) observed beneath the topsoil along the profile.

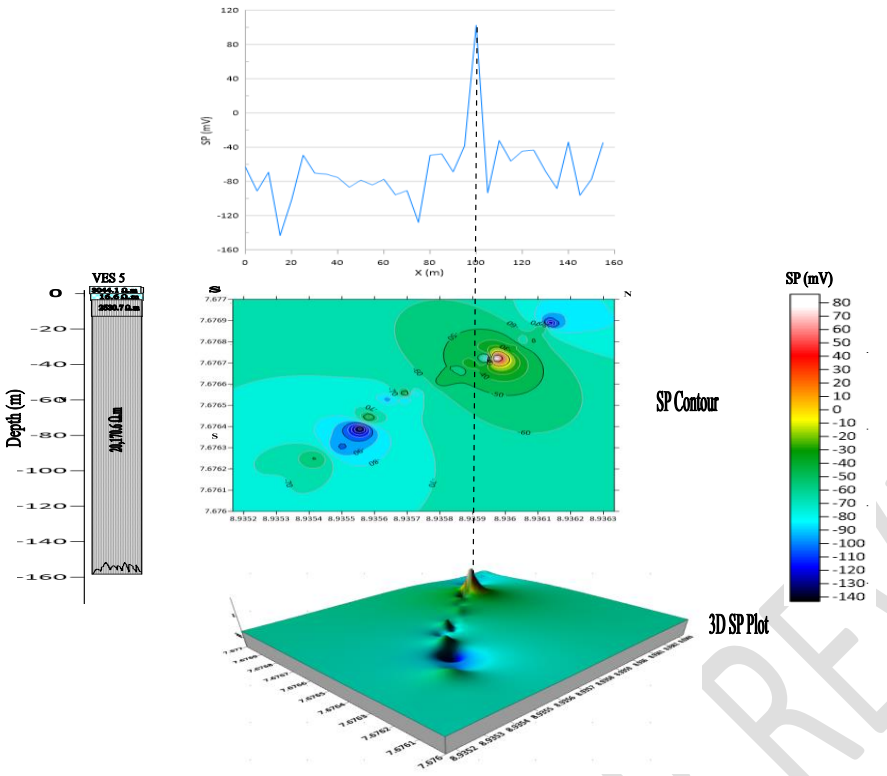

Figure 25: Cross-section correlating the VES transverse, Self-Potential in (mV) signal, SP contours and 3-D SP plot along Profile 5

4.2.6 Discussion

This cross-section (Figure 25) correlates the SP (in mV) profile, VES Log, 2-D SP contours, the 3-D SP plot for profile 5. It shows the variation of positive and negative SP values ranging from (-140 to 90 mV). The undulating variation of the negative SP anomalies ranging from (-140 to -10 mV) peaked at points located between (15 to 20 m), (75 to 80 m) and (130 to 145 m) and it is attributed to leachate infiltration flowing in the N-S direction, along the survey line. This was correlated by the VES log 5 showing materials with low resistivity values of (16.6 Ω.m) extending to depth of 5.5 m along the VES transverse, suggestive of leachate infiltrated zone.

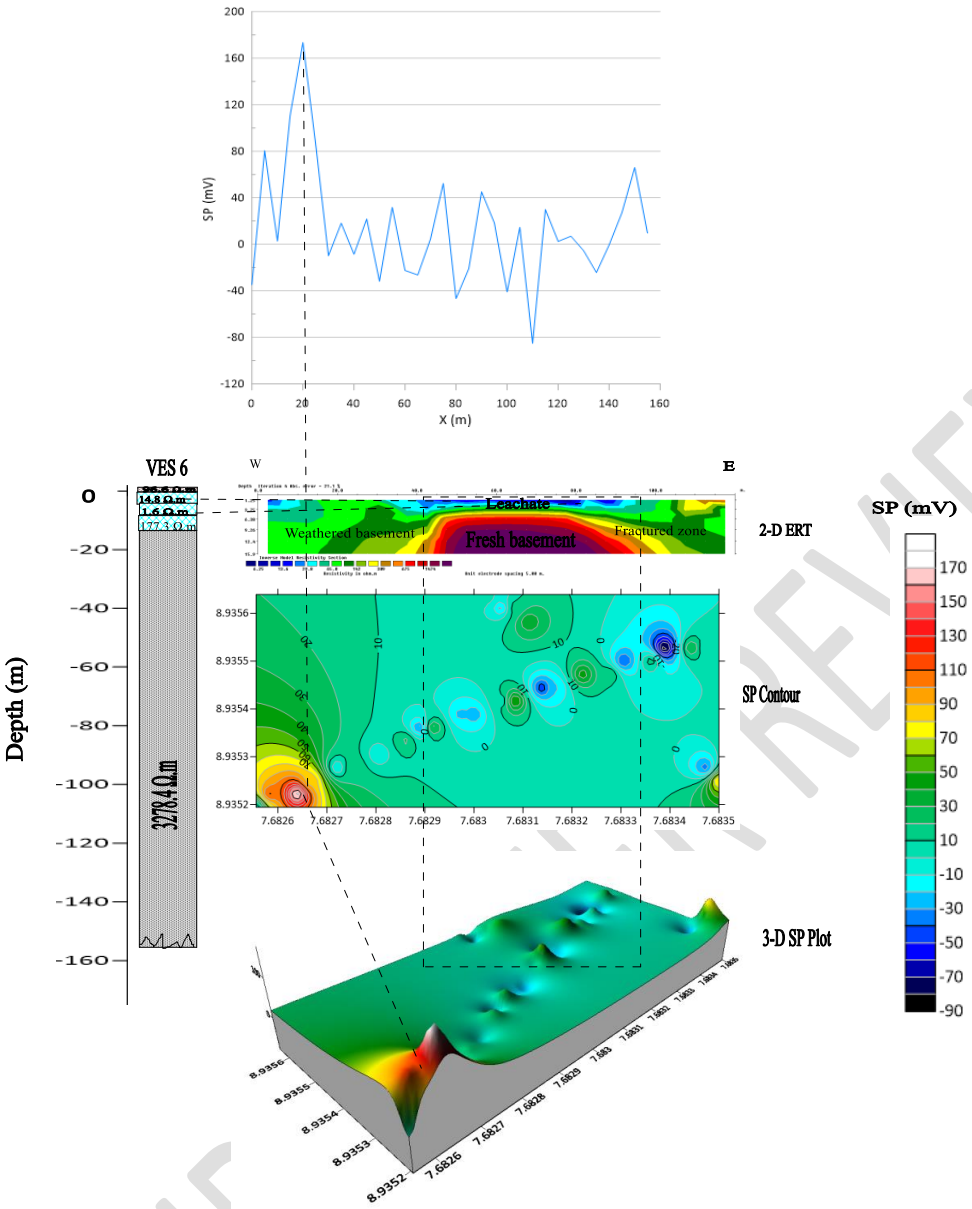

Figure 26: Cross-section correlating the SP profile, 2-D ERT section, VES transverse, SP contour and 3-D SP plot along Profile 6

4.2.7 Discussion

This cross-section (Figure 26) correlates the 2-D ERT, SP contours, 3-D SP plot and SP profile (in mV) and VES log for profile 6. The 2-D ERT line running in the W – E direction. From the southern flank in transverse 2, are materials with low resistivity values ranging from (5.8 to 6.5 Ω.m) extending to depths of 1 to 3.78 m between (0 to 10 m). This is suggestive of areas infiltrated by leachate contaminants. To the northern flank, are materials with similar resistivity values ranging from (5.8 to 6.2 Ω.m) spanning between (40 to 140 m), extending to depths of (0.5 to 3.78 m) interpreted as leachate plumes. The VES log correlated these results with the materials of low resistivity values ranging from (1.6 and 14.8 Ω.m) extending to depths of (4.4 and 9.6 m) in the second and third layers interpreted as leachate infiltrated zone. These were further correlated by

the dominant negative SP values ranging from (-90 to -10 mV) distributed along (40 to 140 m), suggestive of leachate infiltrated zone.

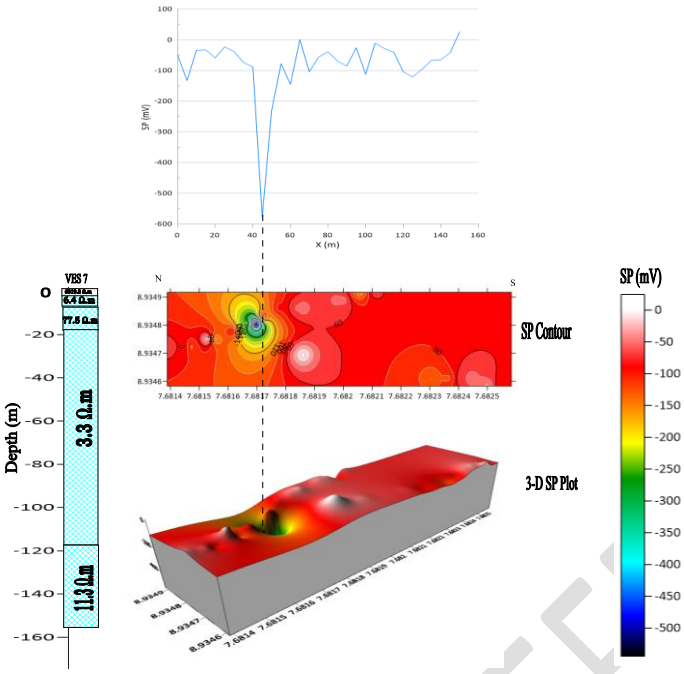

Figure 27: Cross-section correlating the VES transverse, Self-Potential in (mV) signal, SP contours and 3-D SP plot along Profile 7

4.2.8 Discussion

This cross-section (Figure 27) correlates the SP (in mV) profile, SP contours, the 3-D SP plot and the VES log for profile 7. The self-potential values for profile 7 shows dominant negative SP values ranging from (-550 to 0.2 mV) along the entire profile line spanning from (0 to 160 m) in N - S direction. The negative SP values peaked at (-560 mV) between (30 to 40 m) attributed to leachate infiltration into a landfill. This was correlated by the VES log is characterized by materials beneath the topsoil; with low resistivity value of 6.4 Ω.m extending to depth of 8.5 m. The second layer is characterized by a material with resistivity value of (77.5 Ω.m) interpreted as weathered layer. Beyond this layer are materials with very low resistivity values ranging from (3.3 to 11.3 Ω.m) situated between depths of (20 to 157 m) suggestive of leachate infiltrated zone. This profile is interpreted as the most leachate impacted zone within the entire study area. It has been determined that groundwater resources in the area are likely contaminated due to the depth and extent of leachate migration into the subsurface.

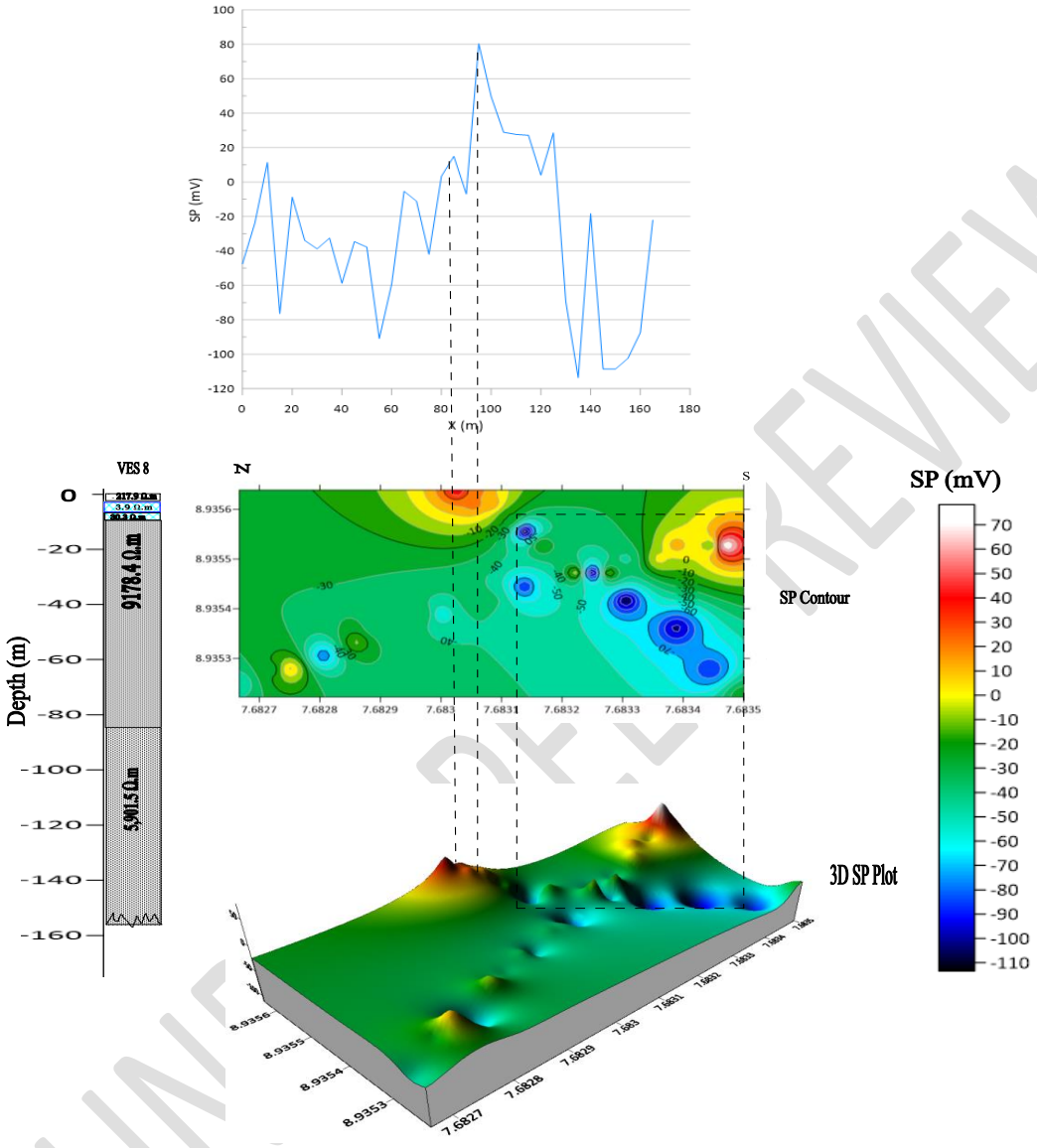

Figure 28: Cross-section correlating the VES transverse, Self-Potential in (mV) signal, SP contours and 3-D SP plot along Profile 8

4.2.9 Discussion

This cross-section (Figure 28) correlates the VES Log, 2-D SP contours, the 3-D SP plot and SP (in mV) signals for profile 1-H running in the North – South direction. The self-potential profile shows variation of positive and negative SP anomalies ranging from (-110 to 80 mV) along profile 8. The negative SP values ranging from (-90 and -110 mV) peaked at points situated between (130 to 150 m), attributed to leachate infiltration zone flowing in the N - S direction, along the profile

line. Also impacted are points located between (10 to 20 m) and (50 to 60 m) with corresponding SP values ranging from (-100 to -60 mV) suggestive of infiltrated leachate zone. These results were correlated by the VES transverse 8 showing materials of low resistivity values ranging from (3.9 to 30.3 Ω.m) observed at depths of (3.7 to 5.7 m) interpreted as leachate infiltrated layers.

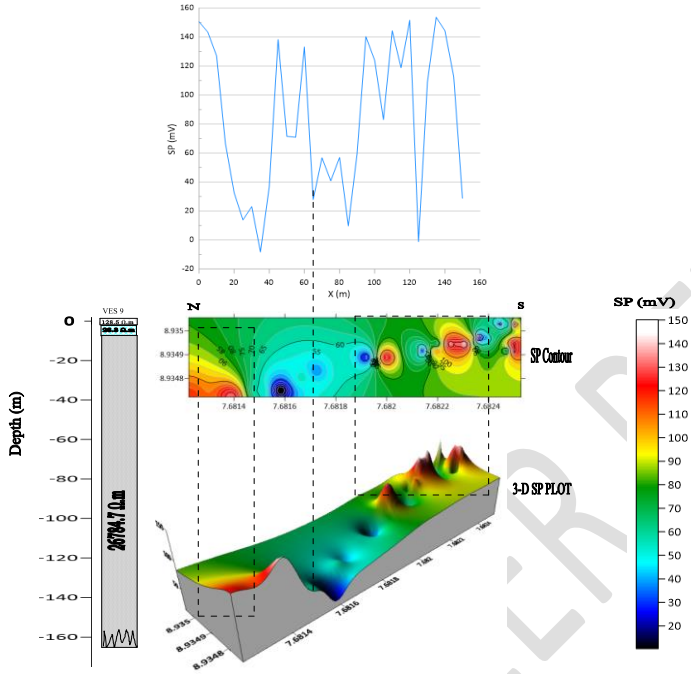

Figure 29: Cross-section correlating the VES transverse, Self-Potential in (mV) signal, SP contours and 3-D SP plot along Profile 9 (Goshen)

4.2.10 Discussion

This cross-section (Figure 29) correlates the VES Log, 2-D SP contours, the 3-D SP plot and SP (in mV) signals for profile 9. The Self-Potential profile 9 shows an undulating section with negative SP anomalies ranging from (-5 to -10 mV) situated between (30 to 90 m) indicative of leachate infiltrated zone. The second layer within VES 9 reveals materials with low resistivity value of 28.3 Ω.m extending to depth of 5.4 m is suggestive of weathered zone.

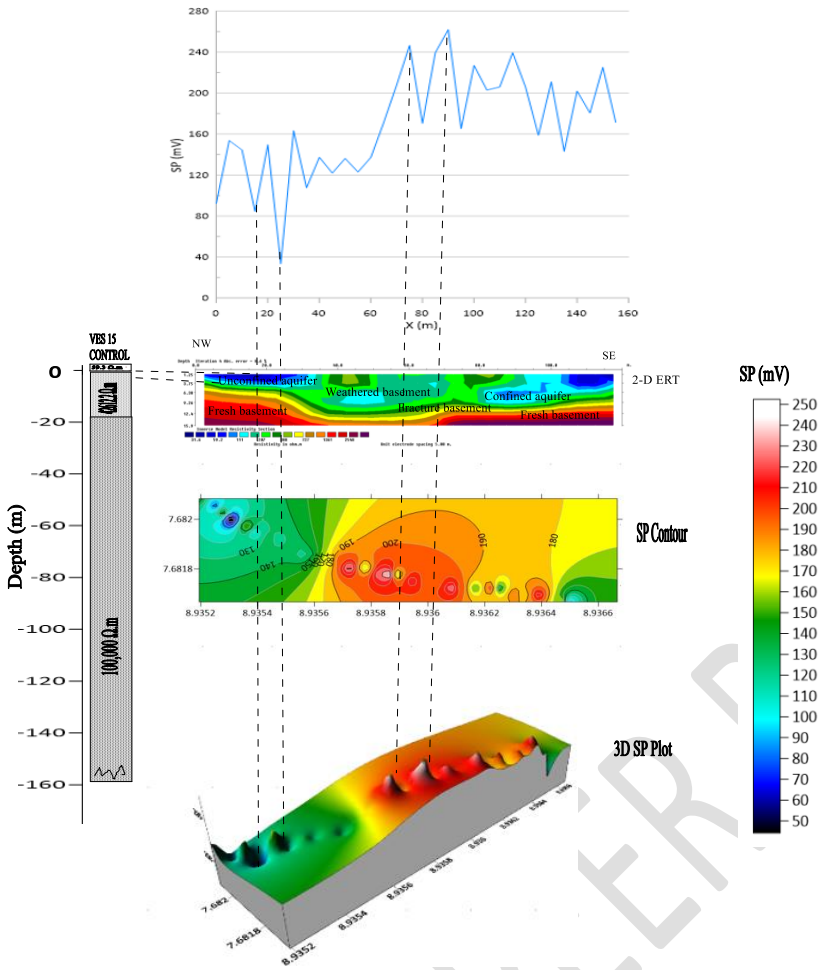

Figure 30: Cross-section correlating the VES transverse, Self-Potential in (mV) signal, SP contours and 3-D SP plot along the Goshen Control Centre

4.2.11 Discussion

This cross-section (Figure 30) correlates the VES Log, 2-D ERT, SP contours, 3-D SP plot and SP profile (in mV) for the Control Centre. The SP profile at the control centre was dominated by positive SP values ranging from (50 to 250 mV) along the entire profile. This established the absence of leachate infiltration into the subsurface. The materials with highest resistivity values ranging from (31.3 to 59.2 Ω.m) recorded along the 2-D ERT section established that the control centre is devoid of leachate contaminants. This is further correlated by the VES results indicating materials with higher resistivity values ranging from (59.3 to 100,000 Ω.m) along the transverse extending to depths of (1.5 to 160 m), providing clear evidence the control centre is leachate free.

4.3 Interpretation of Very Low Frequency Electromagnetic (VLF-EM) results

The results for the nine (9) VLF-EM Transverses 1 - 6 created on the southern part of the dumpsite and transverses 7 to 9 created on the northern part, indicating the fraser filtered, measured VLF and K-H pseudo cross-sections are shown in Figures 31 to 40:

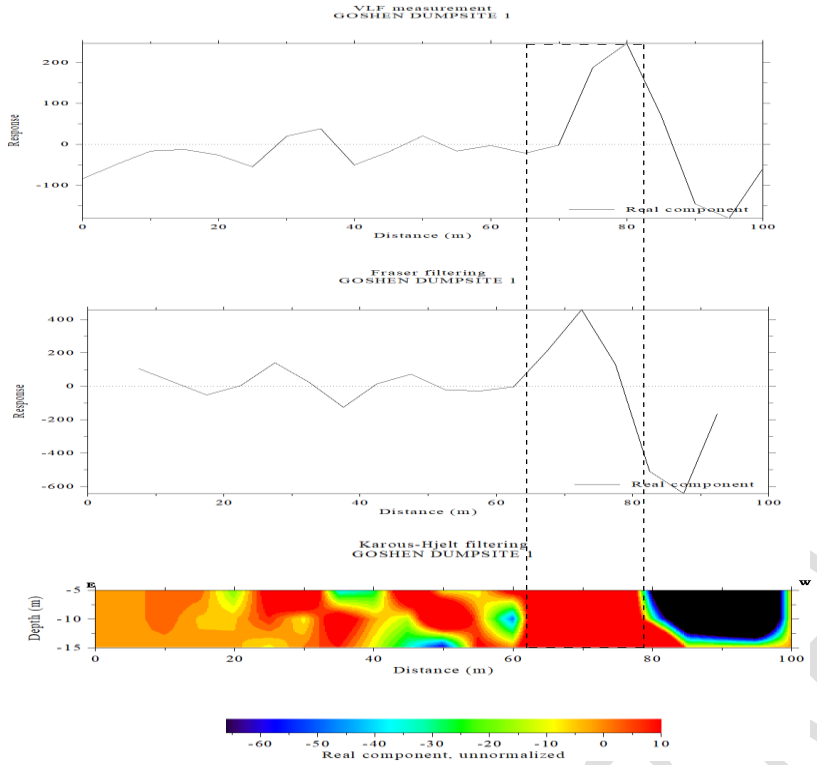

Figure 31: Cross-section of Fraser Filtered, measured VLF and K-H pseudo section along Transverse 1

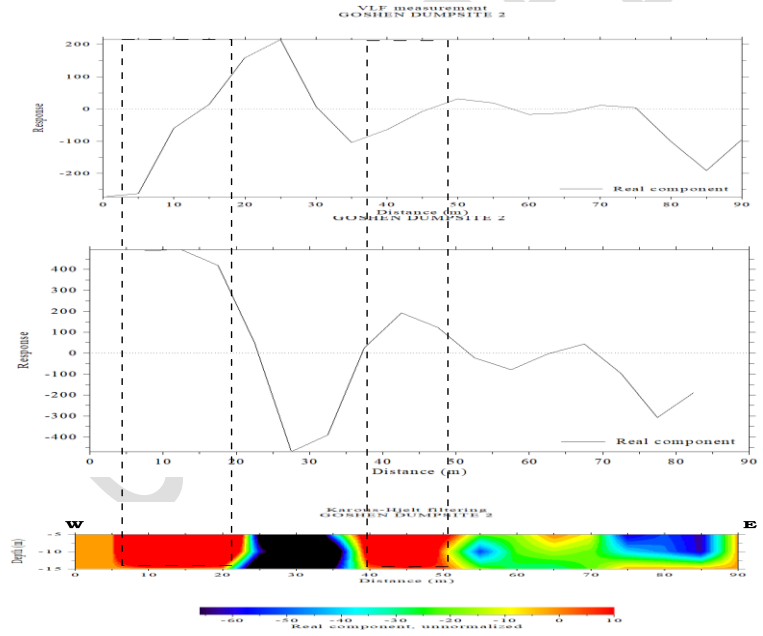

Figure 32: Cross-section of Fraser Filtered, measured VLF and K-H pseudo section along Transverse 2

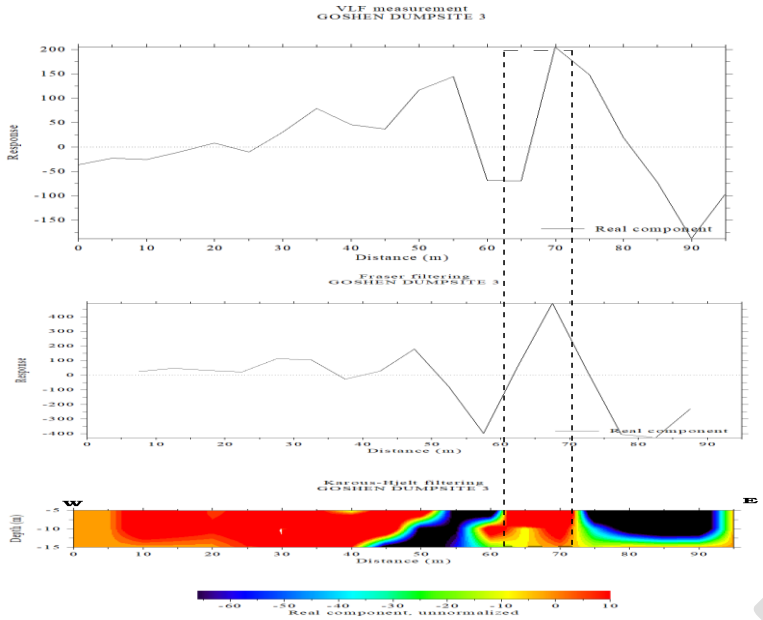

Figure 33: Cross-section of Fraser Filtered, measured VLF and K-H pseudo section along Transverse 3

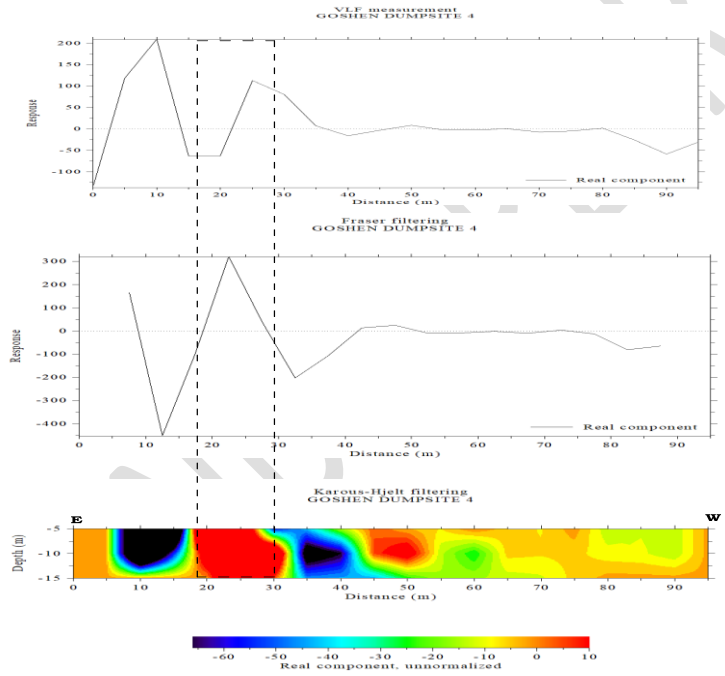

Figure 34: Cross-section of Fraser Filtered, measured VLF and K-H pseudo section along Transverse 4

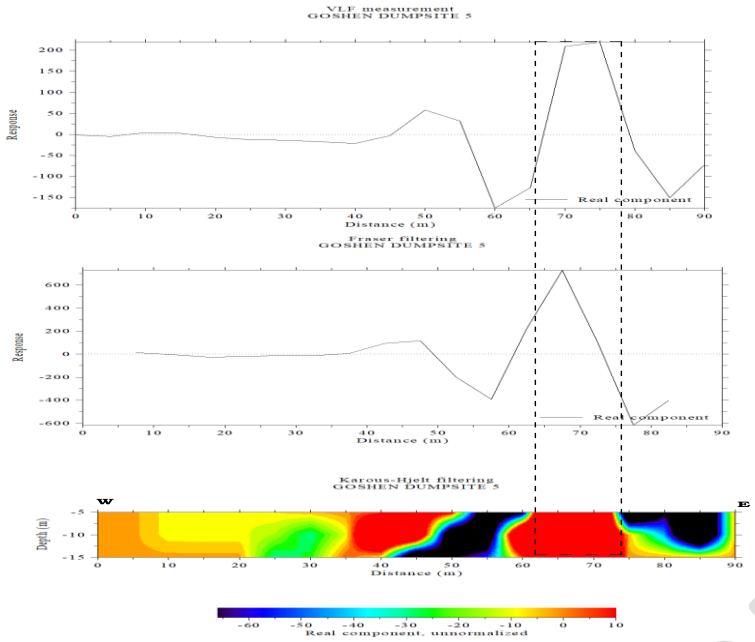

Figure 35: Cross-section of Fraser Filtered, measured VLF and K-H pseudo section along Transverse 5

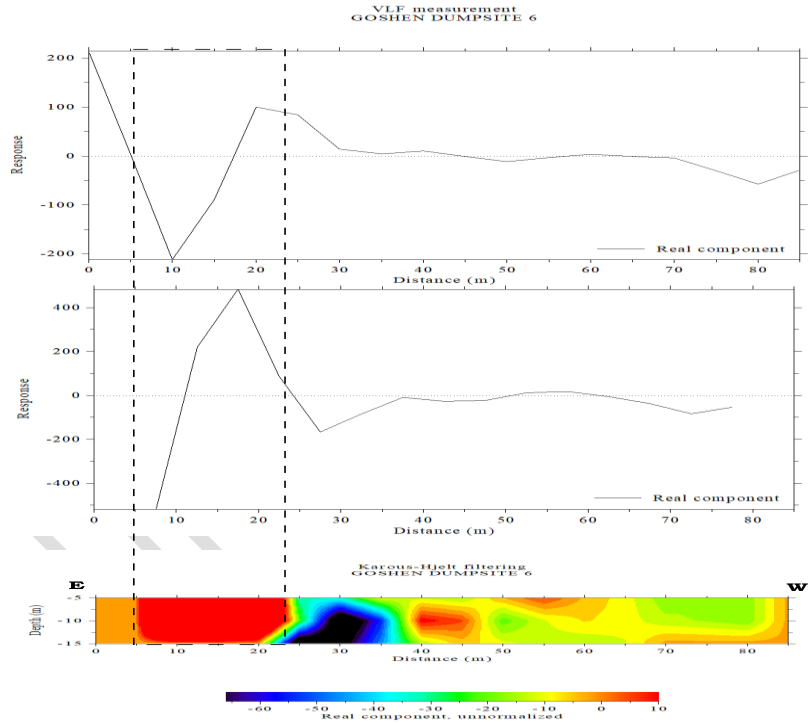

Figure 36: Cross-section of Fraser Filtered, measured VLF and K-H pseudo section along Transverse 6

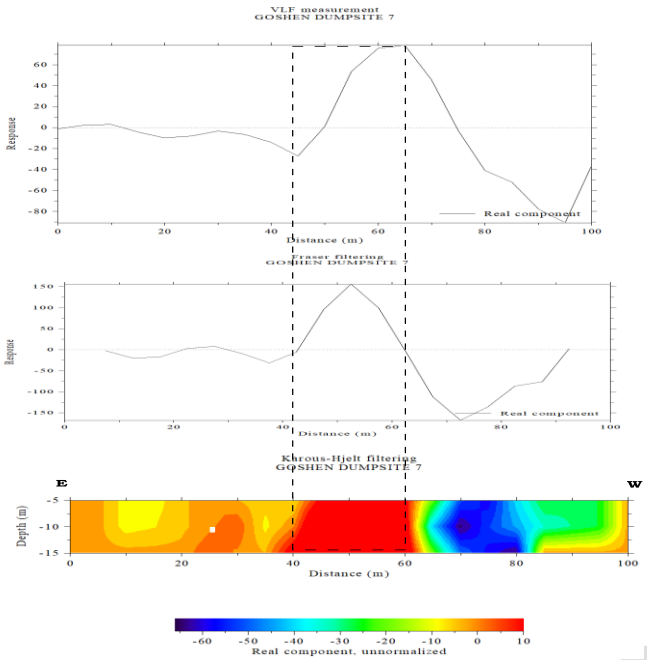

Figure 37: Cross-section of Fraser Filtered, measured VLF and K-H pseudo section along Transverse 7

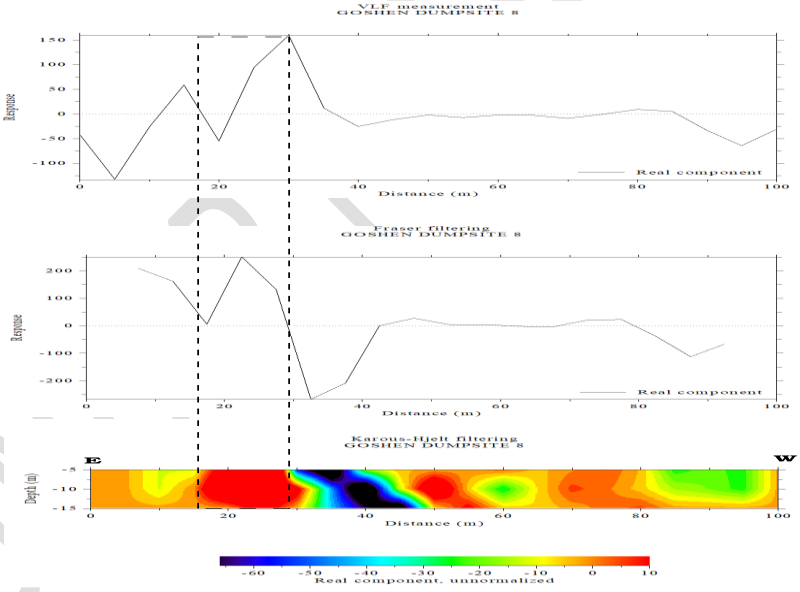

Figure 38: Cross-section of Fraser Filtered, measured VLF and K-H pseudo section along Transverse 8

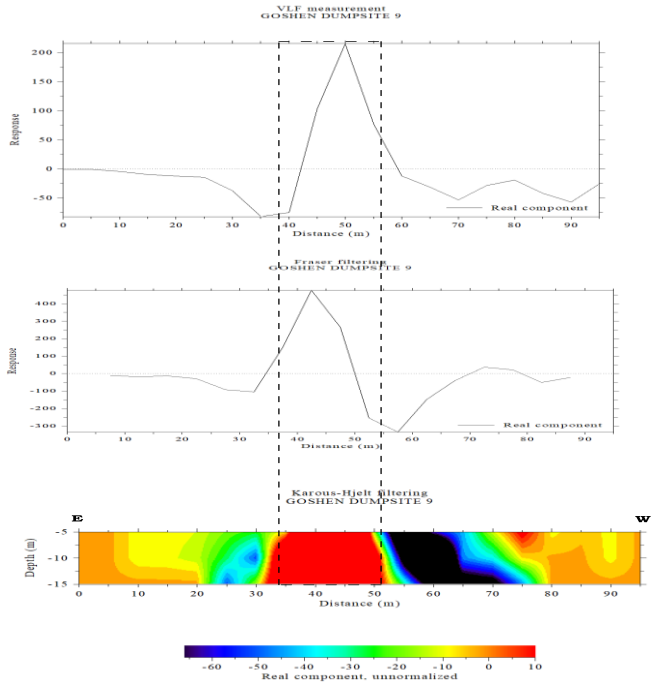

Figure 39: Cross-section of Fraser Filtered, measured VLF and K-H pseudo section along Transverse 9

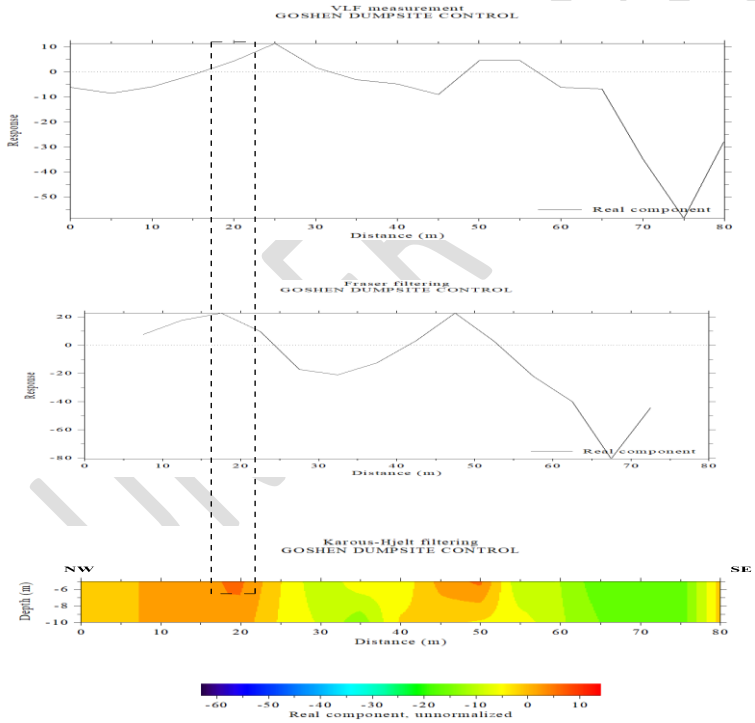

Figure 40: Cross-section of Fraser Filtered, measured VLF and K-H pseudo section along Transverse 10 (Control Centre)

4.3.1 Discussion

4.3.2 Transverse 1

The prominent high positive anomaly ranging from (5 to 10%) between (32 to 51 m) situated along Transverse 1 in the E – W direction, is suggestive of lateral and vertical spread of leachate from the dumpsite into the subsurface. The waste must have generated electrical conducting paths under the subsurface. Between 80 to 100 m is a black material with high negative anomaly ranging from (-50 to -60 %). This is suggestive of mineralized concrete iron sandstone. At distances between (10 to 20 m), (38 to 41 m), (41 to 50 m), are greenish patches suggestive of rock intrusions. The anomalous conductive zones are suspected to be lineament structures while the resistive features are presumed to be lateritic/hardpan/basement formation.

4.3.3 Transverse 2

The high positive anomaly ranging from (5 to 10%) along (8 to 20 m) and (40 to 50 m) along Transverse 2 in the W – E direction is suggestive of migration of leachate contaminant into the subsurface. Between (20 to 40 m) is a black material with negative anomaly ranging from (-50 to -60 %). This is suggestive of pegmatites which outcrops the area. At distances between (50 to 90 m), are intercalations of greenish, bluish and lemon coloured materials suggestive of rock intrusions. The anomalous conductive zones are suspected to be lineament structures while the resistive features are presumed to be weathered bedrock.

4.3.4 Transverse 3

The anomaly (highly positive) ranging from (5 to 10%) along (10 to 40 m) and (60 to 70 m) of Transverse 3 in the W – E direction is suggestive of leachate infiltration. Situated between (40 to 60 m) and (70 to 100 m) are black materials with high negative anomaly ranging from (-50 to -60 %). The anomalous conductive zones are suggestive of lineament structures.

4.3.5 Transverse 4

The prominent high positive anomaly ranging from (5 to 10%) along (20 to 30 m) and (42 to 52 m) extending to depths of (5 to 14 m) along the survey line is suggestive of infiltration of leachate into the subsurface flowing in the E – W direction. Black materials with high negative anomaly ranging from (-50 to -60 %) located between (30 to 40 m) and (5 to 20 m) are suggestive of fractured zone hosting mineralized iron sandstone. The materials consisting of intercalations of lemon, yellowish and orange coloured patches situated between (55 to 100 m) are suggestive of various rock materials. The anomalous conductive zones are suspected to be lineament structures while the resistive features are presumed to be hardpan or basement formation.

4.3.6 Transverse 5

The prominent materials with high positive anomaly ranging from (5 to 10%) situated between (60 to 70 m) and (30 to 40 m) extending to depths of (5 to 15 m) along the survey line in the W – E direction is suggestive of lateral and vertical spread of leachate into the subsurface. The black materials with high negative anomaly ranging from (-50 to -60 %) situated between (40 to 60 m) and (70 to 90 m) are suggestive of fractured zone hosting mineralized pegmatites, while the intercalations of materials with lemon, yellowish and orange coloured patches located between (0 to 30 m) are suggestive of hardpan.

4.3.7 Transverse 6

The materials with high positive anomaly ranging from (5 to 10%) along (5 to 21 m) extending to depths of (5 to 15 m) along the survey line is interpreted as leachate contaminated zone flowing in the E – W direction. The black materials negative anomaly ranging from (-50 to -60 %) between (21 to 35 m) are suggestive are of fractured layer hosting mineralized pegmatites. The materials with intercalations of lemon, yellowish and orange coloured patches, situated between (40 to 100 m) are suggestive of various rock materials.

4.3.8 Transverse 7

The materials with high positive anomaly ranging from (5 to 10%) situated along (40 to 60 m) and (20 to 40 m) extending to depths of (5 to 15 m) in the E – W direction are suggestive of leachate infiltration. The intercalations of lemon, yellowish and orange coloured patches, located between (60 to 100 m) are suggestive of various rock materials.

4.3.9 Transverse 8

The materials with positive anomaly ranging from (5 to 10%) situated along (10 to 28 m) and (45 to 60 m) extending to depths of (5 to 15 m) along the survey line in the E – W direction is suggestive of lateral and vertical spread of leachate from the dumpsite into the subsurface. The greenish circular object situated between (55 to 61 m) is interpreted as hematite intrusion. On the right flank spanning from (60 to 100 m) at depths of 5 to 14 m is another greenish material suggestive of a rock. Between 5 to 15 m is a yellowish material extending to depths of 14 m, interpreted as dolomite.

4.3.10 Transverse 9

The materials in the E-W direction with prominent high current density anomaly ranging from (5 to 10%) along (30 to 50 m) extending to depths of (5 to 15 m) along the survey line is suggestive of leachate infiltrated zone. Between (51 to 80 m) are black materials with high negative anomaly ranging from (-50 to -60 %) suggestive of fractured zone hosting mineralized rocks. Between (0 to 10 m) and (29 to 30 m) are patches of yellowish and orange materials, suggestive of fractured rocks. Between 80 to 100 m are yellowish and orange coloured materials suggestive of pegmatite intrusive rocks.

4.3.11 Transverse 10

The results at the control centre situated 500 m away from the dumpsite revealed that they were materials with lesser current density anomaly ranging from (5 to 6 %) situated along (10 to 20 m) extending to depths of (5 to 15 m) trending in the NW – SE direction. The materials with green, lemon and yellow patches were inferred as weathered/fractured materials hosting groundwater resources. Comparatively, the low positive anomaly recorded at control centre established that the area was not impacted by leachate contamination.

5.1 Conclusion

The geophysical methods identified zones of groundwater saturation and potential contamination pathways (e.g., fractures, faults) within the study areas. The VES and 2-ERT identified four to five discrete geo-electric layers, such as Topsoil consisting of lateritic soil; second layer - interpreted as clayey sand; third layer - inferred as weathered/fractured; the fourth and fifth layers - interpreted

as fresh bedrock. The results revealed that the thickness of the Topsoil (overburden) for the study area ranged from (0.3 to 3 m), with resistivity values ranging from (59.3 to 6103.8 Ω.m). The composition of the overburden was interpreted as low-permeable unconsolidated clay, sandy and gravel materials, which acts as barrier, to leachate infiltration along the transverses. The Aquifer Protective Capacity (APC) rating of the study area was poor to excellent. The results were validated by borehole logs which confirmed that the study area has low to appreciably thick overburden, thus, poor to excellent aquifer protective layers. The materials with low resistivity values ranging from (1.6 to 35.3 Ω.m) along the transverses were interpreted as leachate infiltrated zones. This zones occurred along VES 1 (with resistivity values (7 Ω.m) extending to depths of 2.2 m), VES 2 (19.2 Ω.m, to depths of 3.7 m), VES 3 (35.3 Ω.m , to depths of 4.6 m), VES 4 (17.6 Ω.m, to depths of 3.6 m), VES 5 (16.6 Ω.m, to depths of5.5 m), VES 7 (1.6-14.8 Ω.m, to depths of 9.6 m), VES 8 (3.3 – 11.3 Ω.m, to depths of 123.6 m), VES 9 (3.9 Ω.m, to depths of 3.7 m), VES 10 (28.3 Ω.m, to depths of 5.4 m), VES 11 (20.8 Ω.m, to depths of 3.6 m), VES 13 (12.4 Ω.m, 1.8 m), and VES 14 (13.8 Ω.m, 3.5 m). This result was correlated by the 2-D ERT models indicating that objects with resistivity values ranging from (6.3 to 15 Ω.m) extending to depths of 6.8 m) along VES 2, are suggestive of leachate infiltrated zone. The materials dominated by negative SP anomalies ranging from (-578 to -2.4 mV) within the dumpsites were attributed to differences in mobility and concentration of ions emanating from percolated organic and inorganic materials from the dumpsite. This is in contrast to dominant positive SP anomalies ranging from (1.8 to 247 mV) recorded at the control site. The high positive VLF current-density ranging from (5 to 10%) situated along the transverses were suggestive of leachate generated electrical conducting paths under the subsurface. The materials with negative anomalies ranging from (-50 to -60 %) were interpreted as mineralized rocks within the weathered/fractured layers. To effectively protect shallow and groundwater resources against leachate contamination from the dumpsite, it is recommended that a standard sanitary landfills should be established in the area. It is also recommended that geo-synthetic clay liners be installed at the base of the dumpsites to diminish the rate of leachate percolation into the areafor effective waste disposal management.

DISCLAIMER (ARTIFICIAL INTELLIGENCE)

Author (s) hereby declare that NO generative AI technologies such as Large Language Models (ChatGPT, COPILOT, etc) and text-to-image generators have been used during the writing of this manuscript.

References

1. Abdel-Shafy, H. I., Ibrahim, A. M., Al-Sulaiman, A. M., &Okasha, R. A. (2024). Landfill leachate: Sources, nature, organic composition, and treatment: An environmental overview. *Ain Shams Engineering Journal*, *15*(1), 102293.DOI: https://doi.org/10.1016/j.asej.2023.102293
2. Adeniji, A. A., Ajani, O. O., Adagunodo, T. A., &Kolawole, T. (2024). Investigation of leachate infiltration on groundwater using georesistivity and natural electric field method around Ojoou-Olayanju's dumpsite, Ada, southwestern Nigeria. *Nigerian Journal of Technology*, *43*(1), 159-171. DOI: https://doi.org/10.4314/njt.v43i1.18

3. Arowoogun, K. I., and Osinowo, O. O. (2022). 3D resistivity model of 1D vertical electrical sounding (VES) data for groundwater potential and aquifer protective capacity assessment: A case study. *Modeling Earth Systems and Environment*, 8(2), 2615-2626.
4. Bashir, M. Z. (2018). Geology of The Area Around Kurafe Hausawa, Part of Keffi Sheet 208 nw. 61.
5. Dada, S. S. (2006). Proterozoic evolution of Nigeria. *The basement complex of Nigeria and its mineral resources (A Tribute to Prof. MAO Rahaman). Akin Jinad and Co. Ibadan*, 29-44.
6. Dauda, G., and Ali, A. M. (2024). Delineating leachate-groundwater interaction at Gyadi-Gyadi dumpsite, Kano, using natural electromagnetic (EM) field detector and Vertical Electrical Sounding (VES). *Geosystems and Geoenvironment*, *3*(4), 100303.DOI:https://doi.org/10.1016/j.geogeo.2024.100303
7. de Groot S.R., and P. Mazur, Non-linear thermodynamics. *Dover Publications.* 1983. 510 p.
8. Igwegbe, C. A., López-Maldonado, E. A., Landázuri, A. C., Ovuoraye, P. E., Ogbu, A. I., Vela-García, N., & Białowiec, A. (2024). Sustainable municipal landfill leachate management: Current practices, challenges, and future directions. Desalination and Water Treatment, 100709. DOI: https://doi.org/10.1016/j.dwt.2024.100709
9. Jinadasa, S. and De Silva, R., 2009. Resistivity imaging and self-potential applications in ground water investigations in hard crystalline rocks. *Journal of the National Science Foundation of Sri Lanka* 37(1), pp.23-32.
10. NGSA (Nigeria Geological Survey Agency) 2011. Geological map of Abuja. Published by the Authority of the Federal Republic of Nigeria.
11. Odoh, B. I., Korie, J. I., Arukwe-Moses, C. P., Ahaneku, C. V., Azike, M. C., Muogbo, C. D., &Chibuzor, S. N. (2024). Assessing the Impact of Leachate Infiltration from Dumpsites into the Groundwater System of Agu-Awka and Environs, Southeastern Nigeria. *Journal of Geography, Environment and Earth Science International*, *28*(8), 141-160. DOI: https://doi.org/10.9734/jgeesi/2024/v28i8804
12. Oladapo, M. I., and Akintorinwa, O. J. (2007). Hydrogeophysical study of ogbese south western Nigeria. *Global journal of pure and applied sciences*, 13(1), 55-61.
13. Onicha, A. D., Onwe, J. C., Ngwuta, N. O., Oguma, S., &Jahanger, A. (2024). Attaining sustainable development in Nigeria: the role of solid waste, urbanization and pollution in reducing under-five mortality. *Discover Sustainability*, *5*(1), 357. DOI: https://doi.org/10.1007/s43621-024-00570-2
14. Overbeek J., 1952, Electrochemistry of the double layer, in: H.R. Kruyt (Ed.), Colloid Science, 1, Irreversible Systems, *Elsevier, New York*, pp. 115.
15. Oversby, V. M. (1975). Lead isotopic study of aplites from the Precambrian basement rocks near Ibadan, southwestern Nigeria. Earth and Planetary Science Letters, 27(2), 177-180.
16. Peter, A., Mallam, A., & Abdulsalam, N. N. (2016). Geo-electrical investigation of subsurface water resources in Kutunku, Gwagwalada Area Council, Abuja, Nigeria. *IOSR J. Appl. Physics*, *8*(5), 9-18.

17. Revil, A., and Jardani, A. (2013). The self-potential method: Theory and applications in environmental geosciences. Cambridge University Press.
18. Sanuade, O. A., Arowoogun, K. I., & Amosun, J. O. (2022). A review on the use of geoelectrical methods for characterization and monitoring of contaminant plumes. ActaGeophysica, 70(5), 2099-2117. DOI: https://doi.org/10.1007/s11600-022-00858-9
19. Sill W.R., (1982) Self-potential modeling from primary flows, Geophysics 48 (1983) 76–86. [60] A. Tarantola, B. Valette, Inverse problems quest for information, *J. Geophys.* 501
20. Tanko, I. Y., Adam, M., and Dambring, P. D. (2015). Field features and mode of emplacement of pegmatites of Keffi area, north central Nigeria. *International Journal of Scientific & Technology Research*, 4, 214-229.
21. Udosen, N. I., Ekanem, A. M., & George, N. J. (2024). Geophysical exploration to assess leachate percolation and aquifer protectivity within hydrogeological units at a major open dump in Eket, Nigeria. *Results in Earth Sciences*, *2*, 100022. DOI: https://doi.org/10.1016/j.rines.2024.100022
22. Wikipedia page of the National Space Research and Development Agency Online]: Available at: https://en.wikipedia.org/wiki/National_Space_Research_and_ Development_Agency